UNITED STATES
DEPARTMENT OF THE INTERIOR
GEOLOGICAL SURVEY

HYDROGEOLOGY OF THE STILLWATER GEOTHERMAL AREA, CHURCHILL COUNTY, NEVADA

By David S. Morgan

OPEN-FILE REPORT 82-345

CONTENTS

CONTENTS (Continued)

ILLUSTRATIONS

ILLUSTRATIONS (Continued)

TABLES

TABLES (Continued) Page

CONVERSION OF UNITS

Metric units are used throughout this report, although many of the measurements were made using English units. Thermal parameters are reported in the older, more familiar "working" units rather than in the now-standard SI (Standard International) units. The following table lists metric and equivalent English units, and "working units" and equivalent SI units for the thermal parameters.

Multiply metric units	By	To obtain English units
	Length	
millimeters (mm)	3.937×10^{-2}	inches (in)
meters (m)	3.281	feet (ft)
kilometers (km)	3,281	feet (ft)
	.6214	miles (mi)
	Area	
square meters (m^2)	10.76	square feet (ft^2)
square kilometers (km^2)	247.1	acres (ac)
($10^{10} cm^2$)	.3861	square miles (mi^2)
	Volume	
cubic centimeters (cm^3)	6.10×10^{-2}	cubic inches (in^3)
liters (L)	.2642	gallons (gal)
	3.531×10^{-2}	cubic feet (ft^3)
cubic meters ($(m^3$)	35.31	cubic feet (ft^3)
	8.107×10^{-4}	acre-feet (ac-ft)
cubic hectometers (hm^3)	8.107×10^{2}	acre-feet (ac-ft)
	flow	
liters per second (L/s)	15.85	gallons per minute (gal/min)
	25.58	acre-feet per year (ac-ft/yr)
	Mass	
grams (g)	34.528×10^{-2}	ounces (oz)
Kilograms (kg)	2.205	pounds (lb)

CONVERSION OF UNITS (Continued).

Multiply metric units	By	To obtain English units
Temperature		
degrees Celsius to degrees Fahreheit	°F = 9/5 °C + 32	
THERMAL PARAMETERS		
Multiply "working units"	By	To obtain SI units
Thermal Conductivity		
millicalories per centimeter. second. degree Celsius (10^{-3} cal $cm^{-1}s^{-1}°C^{-1}$)	0.4187	watts per meter degree Kelvin ($W\ m^{-1}°K^{-1}$)
Thermal diffusity		
square centimeters per second ($cm^2\ s^{-1}$)	1.0×10^{-4}	square meters per second ($m^2\ s^{-1}$)
Heat-flow (heat flux density)		
microcalories per square centimeter. second (10^{-6}cal $cm^{-2}\ 5^1$) heat flow unit (hfu)	4.187×10^{-2}	watts per square meter ($W\ m^{-2}$)
Energy		
calories (cal)	4.187	joules (J)
Heat Discharge		
calories per second ($cal\ s^{-1}$)	4.187	watts (W)

ALTITUDE DATUM

The term "National Geodetic Vertical Datum of 1929" (abbreviation, NGVD of 1929) replaces the formerly used term "mean sea level" to describe the datum for altitude measurements. The NGVD of 1929 is derived from a general adjustment of the first-order leveling networks of both the United States and Canada. For convienience in this report, the datum is also referred to as "sea level".

HYDROGEOLOGY OF THE STILLWATER GEOTHERMAL AREA, CHURCHILL COUNTY, NEVADA

By

David S. Morgan

ABSTRACT

The Stillwater geothermal area is directly south of the Carson Sink, the northeastern terminus of the Carson River basin in north-central Nevada. The 518-km^2 study area, which includes alkali flats, salt-desert shrub, irrigated farmland, and marshy wetland, is underlain in downward succession by late Pleistocene Lake Lahontan and Holocene post-Lake Lahontan sediments about 300 m thick, interbedded sedimentary and volcanic rocks of Tertiary and Quaternary age, and pre-Tertiary igneous and sedimentary rocks. The Tertiary and older rocks crop out in eroded fault-block mountains surrounding the area.

The geologic structure is controlled by high-angle northwest to northeast-trending basin-and-range faults. Basin-and-range faulting occured from pre-Miocene to Holocene but probably reached a climax during the Pleistocene, before the advent of late Pleistocene Lake Lahontan. Some of the faults are conduits for the upflow of thermal water from a deep source or sources.

On the basis of test drilling at 14 sites, three primary aquifers, three confining beds, and one marginal aquifer were classified within the upper 70 m of sediments. The complex series of intertonguing sands, silts and clays within this interval probably is characteristic of the entire 300-m thickness of Lake lahontan and post-Lake Lahontan sediments that constitutes the shallow ground-water system. Water-table conditions generally exist to depths of 5-10 m, below which confined conditions prevail.

Within the study area, depth to the water table ranged from 1 to 4.5 m in April 1978. Heads in confined zones between depths of 14 and 152 m ranged from 5.7 m below to 3.6 m above land surface. The increase in altitude of confined

water levels with depth at all but one of the piezometer sites indicates strong upward hydraulic gradients resulting from discharge of water at land surface by evapotranspiration. The upward gradients range from 0.01 to 0.22, about 10-300 times larger than the northward to northeastward lateral hydraulic gradients in the primary aquifers. However, because of the even greater contrast between horizontal and vertical hydraulic conductivities in the near-surface deposits, lateral flow velocities exceed vertical flow velocites throughout most of the study area.

The shallow ground-water system is recharged by infiltrated irrigation water, lateral ground-water influx, precipitation on the adjacent mountains and upland slopes, and upflowing thermal ground water. Of these components, infiltrated irrigation water is by far the largest, so that the quantity of upflowing thermal ground water, the element of primary interest in the study, could not be estimated within reasonably narrow limits by conventional hydrologic-budget methods.

The dissolved-solids concentration of shallow ground water decreases with depth from more than 16,000 milligrams per liter (mg/L) within the unconfined aquifer at depths less than 5-10 m to about 4,000 mg/L in water representing a mixture of thermal and nonthermal water, where the temperature exceeds 47°C. Because the relation between the chemical character of the shallow, nonthermal ground water and the deeper, thermal ground water is the reverse of that commonly found in hydrothermal-convection systems, ionic ratios generally used to evaluate the degree of mixing of thermal and nonthermal ground waters could not be used reliably in the Stillwater area. As a result, the quantity of upflowing thermal ground water was not estimated directly from hydrothermal data.

A heat budget provided the most useful information about the water discharge from the deep, hydrothermal system. The extent and configuration of the near-surface thermal anomaly were determined from temperature-gradient data from

the test wells, aided by a temperature survey at a depth of 1 m made in April 1978. Temperature gradients were used with thermal conductivities to calculate conductive heat flow at depths greater than 10-15 m, the approximate limit of the zone affected by seasonal temperature fluctuations. Thermal conductivities were assigned on the basis of laboratory data for core samples of material similiar to that logged in the Stillwater test holes. Near-surface conductive heat flow was found to exceed 3 heat-flow units (hfu) within an area of 100 km^2 and maximum heat flow measured within the area was about 80 hfu.

Temperatures measured at 1 m correlate reasonably well with both temperatures at 30 m depth and heat flow. The 1-m temperature pattern indicated two areas of high heat flow elongated parallel to a major northwest-trending fault. Thermal and geophysical evidence indicates that the fault conducts thermal water upward into a sand aquifer of probable Tertiary age and into overlying lake sediments.

Heat discharge from the 100-km^2 area of anomalous heat flow (> 3 hfu), 8.2×10^6 cal/s, was computed as the sum of net conductive discharge, 6.5×10^6 cal/s, and convective discharge from wells, 1.7×10^6 cal/s. On the basis of this anomalous heat discharge, assumed to represent the effects of thermal-water upflow from a deep source, and a source temperature of 159°C calculated from chemical geothermometry, water discharge from the hydrothermal system was calculated to be 55 kg/s.

All the evidence indicates that the hydrothermal system is recharged by meteoric water which migrates to depths of 3-6 km along basin-and-range faults, where it is heated to temperatures of 160-240°C by capturing part of the regional heat flow. The thermal water flows upward along one or more fault conduits and then flows laterally in sand aquifers in the Cenozoic deposits.

INTRODUCTION

Objectives and Scope

The objectives of this study of the Stillwater geothermal area were to (1) delineate the near-surface geology, (2) describe the hydrologic environment, (3) define the areal extent and magnitude of anomalous heat flow, (4) determine the source and movement of thermal and nonthermal ground water, (5) obtain a basic understanding of the chemical relationships between the thermal and shallow ground waters and (6) develop a conceptual model of the hydrothermal system. A final objective, which this study had in common with other geothermal studies by the U.S. Geological Survey, was to develop and evaluate efficient and effective reconnaissance methods of geothermal-resource characterization and evaluation. These objectives were attained with various degrees of success, depending on the time, human energy, and resources available for each. The study answers many of the questions concerning the hydrogeology of the Stillwater area, and where no answers were found, serves as a starting point for future work.

The investigation described here was carried out during the fall of 1977 and the first six months of 1978. The area of study (fig. 1) is within the Stillwater-Soda Lake KGRA of the Carson Desert, about 120 km east of Reno, near the small community of Stillwater. Data were collected most intensively in the central part of the 518 km^2 study area, within and immediately adjacent to the thermal anomaly.

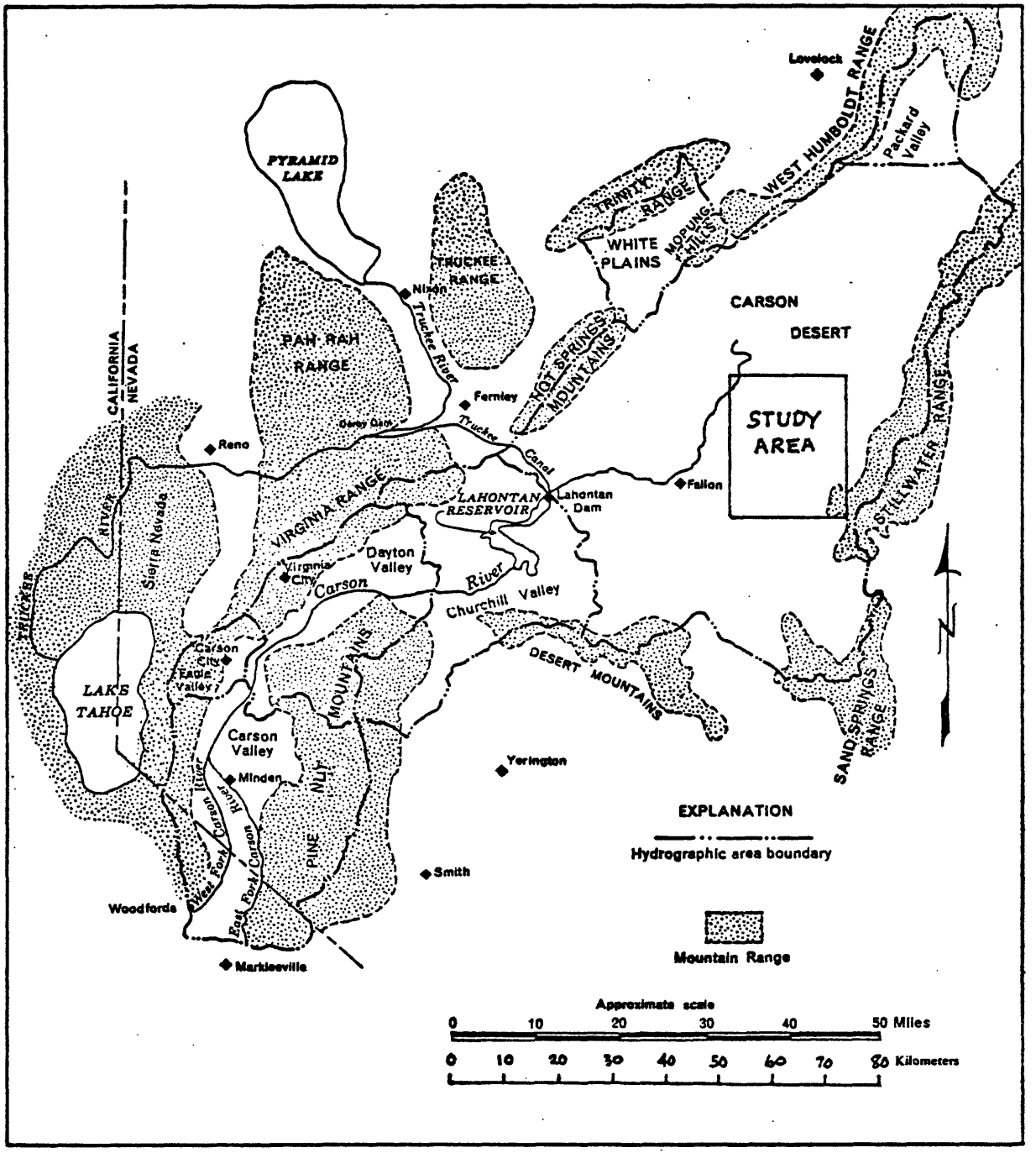

FIGURE 1. -- Index map showing the location of the study area.

Methods of Investigation

The methods used in the study include many of those used by the U.S. Geological Survey in other similar investigations in northern and central Nevada. For example, see Olmsted, Glancy, Harrill, Rush, and Van Denburgh (1975); Presser and Barnes (1974); Sass, Ziagos, Wollenberg, Monroe, de Somma, and Lachenbruch (1977); and Olmsted (1977). As in these earlier investigations, an important objective was the development and evaluation of various reconnaissance methods of studying hydrothermal systems. The techniques used in this study included: (1) collection of existing published and unpublished information; (2) test drilling; (3) borehole geophysical logging, including careful measurement of temperature and temperature gradient; (4) a temperature survey at a depth of 1 m; (5) water-level measurements in test wells and shallow piezometers; (6) sampling and chemical analysis of water; and (7) laboratory analysis of core samples from test wells.

Considerable published and unpublished information was available at the beginning of the study. This information is summarized in the next section, "Previous Work".

Test drilling provided most of the information required for this study. Sixteen test holes were drilled at 14 sites to obtain geologic, thermal, and hydrologic data. Sites were chosen primarily to determine the extent of the hydrothermal discharge area and the magnitude of heat and thermal-ground-water discharge from the area. Depths of the test holes range from 14 to 154 m, but most are less than 60 m deep. The holes were drilled by the mud-rotary method, using a drag bit 124 mm in diameter. At all 14 sites, piezometers ranging in depth from 2 to 5 m were installed by hand auger in order to measure the depth to the water table and, in conjunction with the deeper test holes, to determine the vertical hydraulic gradient. The deeper test holes were completed with

galvanized-steel pipe of 38 or 51 mm nominal inside diameter having a well-point screen 1.2 m in length fitted at the bottom. The shallow piezometers were completed with polyvinyl chloride (PVC) pipe 51 mm in diameter in which slots were cut in the lowermost section over a 50-cm interval.

In addition to the wells and piezometers described above, 10 other test wells ranging in depth from 20 to 45 m were drilled for a previous hydrogeologic study of the area by Olmsted, Glancy, Harrill, Rush, and Van Denburgh (1975). The important difference in the method of construction beween the original set of 10 wells and the 16 wells drilled for the present study, is that the annulus between the casing and the wall of the drill hole was not sealed with cement grout in the original wells as it was in the later 16 wells. As a result, convective heat transport by water moving through the annulus was eliminated or minimized in the 16 wells drilled for this study, and both the temperature profile and the water level probably represent natural conditions in the formation more nearly in these wells than they do in the original wells.

Data on the wells and test holes used in this study are given in table 1.

Seven kinds of geophysical logs were made in almost all the 16 test holes. Available logs include: (1) single-point resistivity; (2) spontaneous-potential; (3) caliper (hole-diameter); (4) gamma (natural-gamma); (5) gamma-gamma (formation density); (6) neutron; and (7) temperature. The uses made of these logs were similar to those described by Olmsted, Glancy, Harrill, Rush, and Van Denburgh (1975) and are not discussed further here.

A temperature survey at a depth of 1 m was made during a four-day period in early April 1978. Measurements were made at 43 sites, mostly within the 14-km^2 area of the highest heat flow, using equipment and methods described by Olmsted (1977) in the nearby Soda Lakes and Upsal Hogback areas. Early April was selected as

TABLE 1.-- Data for test holes and wells in the Stillwater geothermal area, Nevada

Well or test hole number	Location number	Latitude north ° ' "	Longitude west ° ' "	Depth to middle of screen m	Altitude of land surface m	Casing diameter mm	Completion [1]	Water level [2] m	Date yr.mo.da.	Geophysical logs available [3]	Other data [4]
CDDH-101A	20/30-12dad1	39 36 41	118 33 23	30.55	1182.58	51	ST, SC, CM	+3.56	78 04 07	R,Sp,C,G^2,G,N	L,W,C,T
AH-101B	20/30-12dad2	39 36 41	118 33 23	3.06	1182.58	38	PV, SL, BF	-2.7	78 04 07	----------	W
DH-102A	20/31-19cbd1	39 34 59	118 33 06	152.80	1181.41	51	ST, SC, CM	+0.23	78 04 07	R,SP,C,G^2,G,N	L,W,T,O
AH-102B	20/31-19cbd2	39 34 59	118 33 06	1.73	1181.41	38	PV, SL, BF	-1.08	78 04 07	----------	W,C
DH-106A	19/30-14caa1	39 30 33	118 35 05	17.70	1190.51	38	ST, SC, CM	-1.38	78 04 06	R,C,G^2,G	L,W,C,T
DH-106B	19/30-14caa2	39 30 33	118 35 05	51.50	1190.51	51	ST, SC, CM	-0.10	78 04 06	R,G^2,G,N	L,W,T
DH-106C	19/30-14caa3	39 30 33	118 35 05	92.70	1190.51	51	St, SC, CM	+0.33	78 04 06	R,C,G^2,G,N	L,W,T
AH106D	10/30-14caa	39 30 33	118 35 05	4.04	1190.51	38	PV, SL, BF	-2.42	78 04 06	----------	W,C
DH-107A	19/30-23dda1	39 29 44	118 34 32	46.00	1191.71	51	ST, SC, CM	+0.06	78 04 02	R,C,G^2,G,N	L,W,T
AH-107B	19/30-23dda2	39 29 41	118 34 32	2.61	1191.71	38	PV, SL, BF	-3.49	78 04 02	----------	W
DH-108A	19/31-30abb1	39 29 30	118 32 45	26.05	1191.64	38	ST, SC, CM	+0.42	78 04 03	R,SP,C,G^2,G	L,W,C,T,O
AH108A	19/31-30abb2	39 29 30	118 32 45	3.05	1191.64	38	PV, SL, BF	-2.82	78 04 03	----------	W,C
DH-110A	19/31-9bbb1	39 31 03	118 31 03	19.30	1187.76	38	ST, SC, CM	-1.28	78 04 04	R,SP,C,G^2,G	L,W,T
AH-110B	19/31-abbb2	39 31 57	118 31 03	11.03	1187.76	38	PV, SL, BF	-2.02	78 04 08	----------	W,C
DH-111A	19/31-10cbb1	39 31 29	118 29 34	12.20	1190.49	38	ST, SC, CM	-5.27	78 04 05	----------	L,W,C,T,O
AH-111B	19/31-10cbb2	39 31 29	118 29 54	4.04	1180.49	38	PV, SL, BF	-4.28	78 04 05	----------	W

TABLE 1.-- Data for test holes and wells in the Stillwater geothermal area, Nevada (Continued).

Well or test hole number	Location number	Latitude north ° ' "	Longitude west ° ' "	Depth to middle of screen m	Altitude of land surface m	Casing diameter mm	Completion [1]	Water level [2] m	Date yr.mo.da.	Geophysical logs available [3]	Other data [4]
DH-112A	20/31-33cac1	39 33 11	118 30 47	55.10	1185.82	51	ST, SC, CM	+0.31	78 04 05	R,SP,C,G^2,G,N	L,W,T
AH-112B	20/31-33cac2	39 33 11	118 30 47	1.81	1185.82	38	PV, SL, BF	-1.81	78 04 05	----------	W
DH-113A	19/30-1ccc1	39 31 58	118 34 25	48.70	1186.82	51	ST, SC, CM	+0.35	78 04 05	R,C,G^2,G,N	L,W,T,O
AH-113B	19/30-1ccc2	39 31 58	118 34 25	2.41	1186.82	38	PV, SL, BF	-2.26	78 04 06	----------	W
DH-116A	19/30-13bba1	39 31 00	118 34 14	13.50	1189.13	38	ST, SC, CM	-1.50	78 04 02	R,SP,C,G^2,G	L,W,T,O
AH-116B	19/30-13bba2	39 31 00	118 34 14	5.50	1189.13	38	PV, SL, BF	-2.38	78 04 02	----------	W
DH-117A	19/31-7dcb1	39 31 16	118 32 46	19.73	1188.45	51	ST, SC, CM	-0.78	78 04 02	R,SP,C,G^2,G,H	L,W,C,T,O
AH-117B	19/31-7dcb2	39 31 16	118 32 46	3.56	1188.45	38	PV, SL, BF	-3.28	78 04 02	----------	W,C
DH-119A	20/31-31ccd1	39 32 56	118 33 06	17.94	1184.75	51	ST, SC, CM	-0.43	78 04 04	R,SP,C,G^2,G,N	L,W,T,O
AH-119B	20/31-31ccd2	39 32 56	118 33 06	3.98	1184.75	38	PV, SL, BF	-2.69	78 04 04	----------	W
DH-122A	19/31-18bcc1	39 30 37	118 33 14	19.53	1189.74	51	St, SC, CM	-1.67	78 04 07	R,Sp,C,G^2,G,N	L,W,T,O
DH-123A	19/30-12aaa1	39 31 55	118 33 17	37.10	1187.42	51	ST, SC, CM	+1.96	78 04 07	R,SP,C,G^2,G,N	L,W,C,T,O
AH-123B	19/30-12aaa2	39 31 55	118 33 17	3.61	1187.42	38	PV, SL, BF	-3.11	78 04 01	----------	W,C
AH-15A	19/30-10cdd1	39 31 11	118 36 11	45.20	1190.5	38	ST, SC, BF	+0.24	73 04 12	G^2,G,N	L,C,T
AH-16A	19/30-17abb1	39 31 05	118 38 22	45.48	1192.1	38	ST, SC, BF	+0.30	73 04 12	G^2,G,N	L,T

TABLE 1.-- Data for test holes and wells in the Stillwater geothermal area, Nevada (Continued).

Well or test hole number	Location number	Latitude north ° ' "	Longitude west ° ' "	Depth to middle of screen m	Altitude of land surface m	Casing diameter mm	Completion [1]	Water level [2] m	Date yr.mo.da.	Geophysical logs available [3]	Other data [4]
AH-19A	19/31-29ccal	39 28 42	118 31 59	32.9	1196.00	38	ST, SC, BF	-6.81	73 04 13	G^2,G,N	L,T
AH-20A	18/31-6dadl	39 27 04	118 32 10	20.79	1201	38	St, C, BF	----	-- -- --	G^2,G,N	L,T
AH-21A	19/31-29abal	39 29 23	118 31 25	45.48	1191	38	ST, SC, BF	-0.58	73 04 13	G^2,G,N	L,T
AH-22A	20/31-30ccdl	39 33 49	118 33 05	41.18	1183.5	38	ST, SC, BF	+0.46	73 04 14	G^2,G,N	L,T,O
AH-23A	19/30-25dbbl	39 28 58	118 33 52	39.14	1191.8	38	ST, SC, BF	+0.24	73 07 10	G^2,G	L,C,T
AH-24A	19/31-20bbdl	39 30 09	118 32 03	45.42	1190	38	ST, SC, BF	-0.64	73 07 10	G^2,G	L,C,T
AH-25A	20/31-18cbdl	39 35 47	118 33 11	45.26	1182.0	38	ST, SC, BF	+1.22	72 12 16	G^2,G,N	L,T,O
AH-26A	19/31-17cbbl	39 30 42	118 32 08	45.4	1188.4	38	ST, SC, BF	+0.40	73 07 10	G^2,G	L,T,O
OB-01A	19/30-35cbdl	39 27 56	118 35 22	5.2	------	--	-- -- --	-2.93	78 04 14	----------	W
OB-02A	20/30-35ddd1	39 32 58	118 34 30	5.2	------	--	-- -- --	-0.79	78 04 04	----------	W
OB-03A	19/30-9cbd1	39 31 54	118 37 04	6.7	------	--	-- -- --	-1.62	78 04 04	----------	W
OB-04A	19/30-20dcc1	32 29 23	118 38 18	3.0	------	--	-- -- --	-2.13	78 04 04	----------	W
PW-26A	19/31-7dcc1	-- -- --	--- -- --	70.1	------	--	-- -- --	+4.5	78 04 06	----------	C
PW-44A	19/30-6bcb1	-- -- --	--- -- --	56.7	------	--	-- -- --	flowing	78 04 05	----------	C

Footnotes:

[1] ST, galvanized steel tubing; PV, PVC plastic tubing; SC, well point screen; SL, slotted with hacksaw; C, capped at bottom and filled with water; CM, annulus cemented; BF, annulus backfilled with cuttings.

[2] + indicates that water level is above land surface.

[3] R, resistivity; SP, self-potential; C, caliper; G^2, gamma-gamma; G, natural gamma; N, neutron.

[4] L, lithologic log; W, water level data; C, Water quality data (in table); T, temperature log (s); O, one meter temperature.

the optimum time for the survey because, as shown by Olmsted (1977, p. B 4), areal differences in temperature at 1 m resulting from differences in soil-temperature response to seasonal fluctuations in solar-energy input are at a minimum in early April and early October for the climatic and soil conditions at the Soda Lakes and Upsal Hogback thermal areas. Climatic and soil conditions at Stillwater are believed to be similar to those at Soda Lakes and Upsal Hogback.

Water-level measurements in the test wells and shallow piezometers were used to determine the vertical and lateral hydraulic gradients and from these the direction of ground-water flow. Additional water-level information was obtained from four shallow observation wells measured every 2 weeks by the Nevada District office of the Water Resources Division, U.S. Geological Survey. The Lahontan Projects Office of the U.S. Bureau of Reclamation provided water-level records for several water-table piezometers installed as part of an engineering study near Stillwater Point Reservoir. Techniques used for the measurements and for analysis of the data were similar to those described by Olmsted, Glancy, Harrill, Rush, and Van Denburgh (1975, p.40-42).

Water samples from 13 wells and one irrigation canal were collected and analyzed as part of this study. After development of the wells by air-lift pumping or bailing until specific conductance and temperature of the water remained constant (so as to insure that the sample subsequently collected represented unmodified formation water), a 1.5-L sample was run through a filter with a pore size of 45 μm. Of the filtered sample, 500 mL was acidified for cation analysis, 500 mL was bottled "as is" for anion analysis, and 200 mL was used for carbonate-bicarbonate field titration and pH measurement. The samples were then sent in sealed polyethylene bottles to the Central Water Quality Laboratory of the U.S. Geological Survey in Arvada, Colorado. Analyses included all the major anions and cations (HCO_3, SO_4, Cl, K, Na, Ca, Mg), and silica (SiO_2), lithium (Li),

boron (B) and arsenic (As). In addition, Robert Mariner of the U.S. Geological Survey in Menlo Park, California analyzed for rubidium (Rb) in 7 samples.

To supplement the data listed above, chemical analyses of water samples from local domestic wells were obtained from the Nevada State Department of Consumer Health, the Desert Research Institute at the University of Nevada-Reno, and the Nevada District office of the Water Resources Division of the U.S. Geological Survey.

The chief purpose of the water sampling and analysis was to determine whether thermal ground water could be distinguished from nonthermal ground water on the basis of chemical differences, and if so, the degree and mechanism of mixing the two waters, as well as estimated reservoir temperatures.

During the test-drilling program, 14 cores were taken to provide data on the geologic, hydraulic, and thermal properties of the deposits penetrated in the Stillwater area. Analyses were done by the Materials Testing Laboratory of the College of Engineering, University of California, Berkeley, directed by W. H. Somerton, and included determination of saturated bulk density, dry bulk density, porosity, and thermal conductivity. In addition, the cores, which were taken in steel tubes and sealed at both ends by air-impermeable tape and paraffin were later examined megascopically by the writer, and thermal conductivity of three of the cores was measured by Robert Munroe of the U.S. Geological Survey Geothermal Laboratory in Menlo Park, California. As will be discussed later in the section, "Thermal Conductivity of the Materials" (p. 70), the measured values of thermal conductivity were not used directly to determine conductive heat flow. Instead, values were assigned to the various categories of materials described in the interpreted well logs, chiefly on the basis of earlier work in the area (F. H. Olmsted, written communication, 1978).

Previous Work

Prior to this investigation, Olmsted, Glancy, Harrill, Rush, and Van Denburgh (1975) examined the geothermal hydrology and geology of the Stillwater area as part of a reconnaissance study of several geothermal systems in northern and central Nevada. The Stillwater area was also included in a more general water-resources appraisal of the Carson River basin by Glancy and Katzer (1975). Stabler (1904) reported on the ground water of Carson Sink, showing depth to water and analyses for several hundred samples of ground water. Areal geology was mapped by Morrison (1964) and numerous well logs and stratiqraphic sections are presented in Morrison (1959). The University of Utah Research Institute (1979b, 1979c) has published technical data on a deep geothermal test weill near Stillwater. Other deep subsurface information was available from the O'Neil-Oliphant Reynolds #1 geothermal test well. This information was supplemented by unpublished detailed surface geophysical surveys covering most of the thermal anomaly. More recent geophysical work included a magnetotelluric study by Stanley, Wahl, and Rosenbaum (1976),a detailed gravity study by Grannell (written communication, 1978), and seismic-reflection data released through the University of Utah Research Institute (1979a). Detailed soil mapping has been done by the U.S. Department of Agriculture (1977) in which engineering, agriculture , and recreational suitability was evaluated for each soil type.

Acknowledgements

The cooperation of the following agencies and individuals is appreciated: The Fallon office of the U.S. Fish and Wildlife Service, which provided data on the ecology of the Stillwater Wildlife Management Area and assisted in preparing the Environmental Impact Analysis for the test drilling; the Carson City office of the U.S. Bureau of Reclamation, which supplied water-level data for several piezometers near Stillwater Point Reservoir; and the land owners near Stillwater, who allowed access to their property.

Special thanks are reserved for Franklin H. Olmsted of the U.S. Geological Survey, Menlo Park, California, for his advice and consultation throughout the study. Others from the U.S. Geological Survey in Menlo Park who provided valuable assistance include Glenn Blevins and James Robison, who assisted with test drilling and geophysical logging. Valuable assistance was also received from Patrick Glancy, A. S. Van Denburgh, and James Harrill of the staff of the Nevada District office of the U.S. Geological Survey in Carson City.

Well-numbering System

For this investigation wells and test holes were assigned two numbers: A location number referred to the Mount Diablo baseline and meridian, and a chronological number giving pertinent information about the well. The first two elements of the location number are township (north) and range (east), separated by a slash. These are followed by a hyphen and a third number indicating the section number (1-36). The section number is followed by up to three lower-case letters (a, b, c, d) which give the successive quadrant subdivisions of the section. When more than one well or test hole is located within the smallest designated quadrant, the last lower-case letter is followed by a numeral designating the order in which the well was catalogued. The map location of location number 20/61-1cba1 is shown in figure 2.

The chronological number assigned to each well or test hole was intended to give several types of information: the agency that drilled the well, the area of the study, the method of drilling, the order of drilling within the study area, and the order of drilling at the site. A typical chronological number is of the form, USGS CD DH-102A. USGS refers to the U.S. Geological Survey which contracted the drilling of the test holes for this study; CD indicates that the test hole is in the Carson Desert; DH indicates a drill hole, whereas an auger hole designated AH; 102 is the site number. Note: site numbers for test holes drilled during this study begin with 101 so as to be easily distinguished from USGS test holes drilled for the study by Olmsted, Glancy, Harrill, Rush, and Van Denburgh (1975), which have numbers less than 100. The letter "A" indicates the first test hole drilled at site 102. Both the location and chronological numbers are identical in format to well numbers used by the U.S. Geological Survey throughout Nevada. Well numbers prefixed only by PW are privately owned wells.

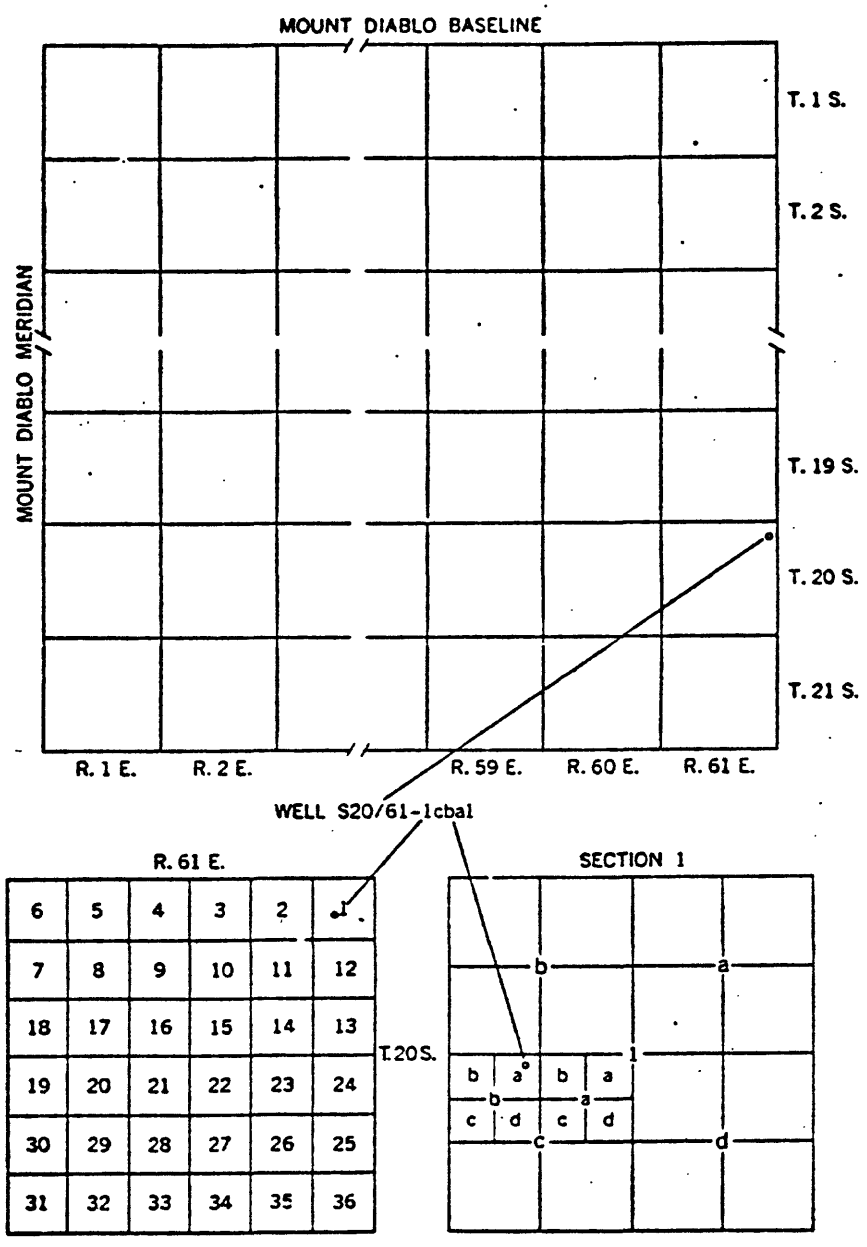

FIGURE 2. -- Well-numbering system.

REGIONAL SETTING

Location and Development

The study area (pl. 1) lies within the Carson Desert in north-central Nevada between lat. 39°25' and 39°40' N., and long. 118°25' and 118°40' W. (See fig. 1). The area is bounded on the north by the Carson Sink, the northeastern terminus and ultimate discharge area of the Carson River basin. The small farming community of Stillwater is situated in the south-central part of the study area, about 20 km east-northeast of Fallon. Stillwater is one of the oldest communities in western Nevada. Historic files contain descriptions of its borax and soda processing plants which provided basic chemicals to ore reduction mills during the 1880's. The Nevada Reclaimation Project (Newlands Project) was authorized under the Reclamation Act of June 17, 1902, and the Stillwater area began receiving irrigation waters in 1905. Subsequently, agriculture has been the main industry of the area with the total irrigated acreage divided nearly equally between alfalfa and pasture. Other crops include hay, barley, and wheat.

A major part of the area of investigation is included in both the Stillwater Wildlife Management Area and the Stillwater National Wildlife Refuge. These areas were withdrawn from the Newlands Project in 1948. The areas are operated, maintained, and developed by the U.S. Fish and Wildlife Service through a cooperative agreement with the Nevada Department of Fish and Game. During optimum water years the area has provided nearly 93 km^2 of wetland habitat for migratory waterfowl. However, in 1974 the habitat varied between 34 and 49 km^2 because of reduced water receipts. (See U.S. Fish and Wildlife Service, 1978.) Habitat has been further reduced in recent years.

Hot-water wells have long been used to heat homes in the area; but, only within the last 15 years has there been commercial interest in Stillwater's geothermal resources. This interest has intensified within the last 5 years and the rights to geothermal steam and hot water have been leased on most of the private land in the

area. The wildlife management area is closed to geothermal development; however, active exploration in the form of deep drilling and geophysical studies is being done on the adjacent private lands.

Regional Geology

The study area lies within the Great Basin, in the western part of the Basin and Range physiographic province. The Carson Desert is the largest intermontane basin in northern Nevada; elongated 112 km in a northeast-southwest direction, it ranges in width from 13 to 48 km. Most of the Carson Desert is below an altitude of 1,220 m. The lowest part of the basin is the Carson Sink, a playa 32 km in diameter at the northern end of the basin at an altitude of 1,172-1,186 m. The sink is nearly flat, completely barren, and in many places, salt-encrusted. It is bounded on the north, west, and east by the piedmont slopes of the surrounding mountains. The lowlands adjacent to the Carson River flood plain consist of sand plains and clay flats. Near the town of Fallon three volcanic hills rise above the lowlands: Rattlesnake Hill and the rims enclosing Soda Lakes and Upsal Hogback. To the east, the Stillwater Range rises abruptly from the desert floor to altitudes of as much as 2,679 m at Jobs Peak. The Lahontan, Bunejug, Cocoon, White Throne, Desert, Dead Camel, and Hot Springs Mountains border the southern and western boundaries of the Carson Desert.

The study area is underlain in downward succession by Holocene post-Lake Lahontan and interbedded eolian and fluvial sediments, interbedded sedimentary and volcanic rocks of Tertiary and Quaternary age, and pre-Tertiary igneous and sedimentary rocks. The sediments of Lake Lahontan and post-Lake Lahontan age are about 300 m thick and constitute the shallow ground-water system of primary interest in the present study.

Pre-Quaternary geologic history is not well documented in the Carson Desert. The following summary has been drawn from the work of Grannell (written communication, 1978) and Morrison (1964). The oldest rocks exposed in the area, in the northern Stillwater Range, consist of Triassic and Jurassic sedimentary rocks extensively intruded by Jurassic and Cretaceous plutons. The oldest Tertiary rocks in the area, in the southern Stillwater Range, consist of minor amounts of flow andesite and associated breccia. Silicic plutonic rocks and rhyolitic intrusive rocks (probably of common magmatic origin) are associated with the older andesites. The intrusive rocks may be as young as Oligocene (?) compared to an age of late Eocene (?) for the flow rocks. The andesite flows are commonly highly altered and sheared.

Overlying these rocks are a series of welded and non-welded ash-flow tuffs which in turn are overlain by a thick sequence of Miocene tuffaceous sedimentary rocks containing local tuffs and rhyolite flows. These rocks can be traced to the Soda Lakes area, but are absent to the north near Desert Peak. This has led to postulation by Grannell (written communication, 1978) that the Stillwater-Soda Lakes area is within a long-existing basin already present in Miocene time. Following this period of silicic volcanism and sedimentation, olivine basalts issued from fissures and pipe-like structures, forming an extensive cap rock for the underlying sediments. Major uplift and block faulting closely followed the basaltic volcanism and formed the present-day basin-and-range topography of the Carson Desert. Alluviation and colluviation in the highlands, valley erosion in the mountains and relative structrual stability were characteristic of the area until the late Pleistocene. Basaltic eruptions at Rattlesnake Hill near Fallon have been dated using the K-Ar method at 1.03 $\pm$ 0.05 million years (my) (Sibbett, 1979, p. 6).

Whereas pre-lake Lahontan history is fragmentary, Lake Lahontan and post-lake Lahontan history is fairly complete. Morrison (1964) has studied this history

extensively and drawn the following conclusions. Lake Lahontan was possibly preceded by an older lake and a period of desiccation. This desiccation was followed by two deep-lake cycles, during which as much as 90 feet of lacustrine gravel, clay, and tufa were deposited, separated by alluvium and colluvium deposited between the lake cycles. Later, the basin was alternately dry and occupied by shallow lakes. Deposition consisted of eolian sand, alluvium, and shallow lake sand and clay. Another lake cycle during which there were three lake maxima and two recessions, deposited intertonguing lacustrine and subaerial sediments. The last recession, near the end of the Pleistocene, was followed by an arid interval when the Carson Desert was completely dry. Morrison (1964) recorded five climatic intervals within the last 4,000 years that were somewhat wetter and cooler than now, when many small lakes occupied parts of the basin floor.

Regional Hydrology

Its moderate altitude and location in the rain shadow of the Sierra Nevada make the Carson Desert one of the warmest and driest areas in northern Nevada. The climate is one of extremes, with wide seasonal and diurnal variations in temperature as well as large areal variations in annual precipitation. Clear, windy days are common and consequently, evaporation is high.

Average annual precipitation within the Carson Desert ranges from less than 100 mm in the Carson Sink to more than 400 mm in the highest part of the Stillwater Range (Hardman, 1965). Annual precipitation at Fallon averages about 130 mm/yr, but fluctuates from as little 50 mm/yr to as much as 200 mm/yr (from published records of the National Oceanic and Atmospheric Administration, NOAA). Most precipitation occurs between December and May, but some falls during intense storms of short duration at other times of the year.

Temperature at Fallon during the period 1903-1951 averaged -1.2^{o}C for January and 23.4^{o}C for July. The maximum extreme range was 55^{o}C and the mean annual

temperature was 10.4°C (from NOAA). Growing seasons typically last 125 days with the first frost coming in early fall and the last in late spring. Average wind velocities are low (less than 8 km/hr); however, brief, violent windstorms are common in spring and early fall. These winds redistribute large volumes of dust and sand; visibilites are often reduced to less than 1 km. Low humidity, as well as high temperatures and winds, accounted for a mean class A pan evaporation rate of 1,742 mm/yr between 1971-1975 (Guitjens and Mahannah, 1976).

The East and West Forks of the Carson River have their headwaters high in the Sierra Nevada, south of Lake Tahoe. At the base of the mountains, in the Carson Valley, the forks join to form the main river. The Carson River is depleted by an average of 156 hm^3/yr by agriculture withdrawals in the Carson Valley. Average releases from Lahontan Reservoir (1919-1969) are 469 hm^3/yr of which 12 hm^3/yr is diverted from the Truckee River to Lahontan Reservoir via the Truckee Canal, table 12 (Glancy and Katzer 1975). Of the Carson River's 10,347 km^2 of drainage area, 5,680 km^2 lies below Lahontan Dam, the river's point of entry into the Lower Carson River basin. Occasionally the basin receives surface-water inflow from the Humboldt River when it overflows Humboldt Lake through the White Plains playa to the Carson Sink. Outflow from Lahontan Reservoir irrigates more than 364 km^2 and the waste water from this irrigation feeds Carson Lake, Stillwater Point Reservoir, Carson Sink, the Indian Lakes, and the Stillwater Lakes. The Stillwater Lakes have the largest surface area, consisting of many interconnected ponds, lakes and intervening marshes. The lakes are fed by Stillwater Slough and other canals of the reclamation project. During the mid-1800's the Carson Sink held a permanent lake; however for the past several decades it has been dry.

Until the development of irrigated agriculture in the lower part of the basin, the Carson River was the main source of water supply and ground-water

recharge. Now, irrigation water penetrating to the saturated zone and leakage from unlined canals are the main source of recharge. An unknown amount of this irrigation water went into ground-water storage between about 1905 and 1930 when local water levels rose by as much as 15-20 m (Rush, 1972). More than half the annual releases from Lahontan Reservoir probably penetrate to the saturated zone before being discharged by evapotranspiration (Olmsted and others, 1975). This source of recharge represents at least 150 times the estimated potential ground-water recharge from the surrounding mountains of 1.6 hm^3/yr (Glancy and Katzer, 1975).

The net lateral movement of ground water is generally northeastward and northward toward the Carson Sink. Sandy aquifers within a few tens of meters of land surface carry most of the water. Deeper, confined ground water moves slowly and has a strong vertical component of flow as it approaches the Carson Sink.

GEOLOGY

Physiography

Physiographically, the study area is representative of the Carson Desert as a whole. Altitudes range from about 1,180 m in the wetlands, sand hills, and clay flats of the north, to 1,661 m in the Lahontan Mountains and west flank of the Stillwater Range in the south and southeast. Between the wetlands and the mountains lie the irrigated farmlands surrounding the community of Stillwater. This area lies within a shallow trough which strikes about N 15^{o} E and slopes gently toward the Carson Sink.

The wetlands consist of two tracts of small lakes and ponds--the Indian Lakes to the west and the Stillwater Lakes to the east. Separating the two wetlands is an area of clay flats which extend from the northern edge of the irrigated land toward the Carson Sink. In the northern part of the study area, the featureless clay flats give way to low sand hills and ridges. The sand ridges are generally alined along a north to northeast strike, and may indicate buried fault scarps. South of the irrigated farmland the desert floor slopes gently upward to the base of the Lahontan Mountains and the piedmont slopes of the Stillwater Range.

Hydrogeologic Units

The study area is underlain in downward succession by late Pleistocene Lake Lahontan and Holocene post-Lake Lahontan sediments about 300 m thick, interbedded sedimentary and volcanic rocks of Tertiary and Quaternary age, and pre-Tertiary igneous and sedimentary rocks. The Lake Lahontan and post-Lake Lahontan sediments underlie the valley; the Tertiary and older rocks crop out in eroded fault-block mountains surrounding the area. Primary emphasis in the present study was placed on the upper part of the Lake Lahontan and post-Lake Lahontan sediments, which are discussed in the following paragraphs.

The near-surface (0-70 m) lacustrine and subaerial sediments of Lake Lahontan and post-Lake Lahontan time were subdivided into three categories on

the basis of gross hydrogeologic properties.

The many modes and environments of deposition in the basin have created a complex series of intertonguing sand, silt, and clay beds with scattered layers of tufa and volcanic ash. Upon examination of drillers' logs, drill cuttings and cores, and geophysical logs, seven major hydrogeologic zones were indentified within the upper 70 m. These zones fall into three categories: (1) units designated as "primary aquifers" consisting predominantly of fine- to medium grained eolian, alluvial, or shallow lake sand together with localized zones of clayey sand and minor clay beds; (2) units considered as "marginal aquifers" consisting primarily of sandy to silty clay with intertonguing beds of fine- to medium-grained sand partings and of volcanic ash; and (3) units functioning as confining beds and consisting predominantly of lacustrine clay and silty and sandy clay and infrequent sand stringers. The seven hydrogeologic units are described below in the approximate order in which they would be encountered by a borehole near the center of the study area. The units and their stratigraphic relationships are illustrated on plate 2. Where possible, correlations are suggested between the hydrogeologic units of this report and lithologic units described and mapped by Morrison (1964).

Marginal Aquifer (MA-1)

Marginal Aquifer (MA-1) is widely exposed, reaching a maximum thickness of 10 m in the central part of the area and thinning to the north and south. It is comprised of beds of calcareous clay, silty to sandy clay, tufa, and medium to fine-grained sand which vary greatly in vertical and lateral extent. Beds of dark organic clay less than 0.5 m thick commonly underlie the sand beds. The carbonate tufa layers were easily indentifiable during the drilling by excessive drill-bit "chatter" and mushy white globules in the cuttings that effervesced when tested with acid. These deposits correspond closely to the Holocene Fallon Formation and the underlying upper member of the Quaternary

Sehoo Formation. The upper sediments would thus record the five Holocene lake cycles, during which shallow lake clay and silt were deposited, and the intervening intervals of lake recession which saw the deposition of alluvial and eolian sand. Much eolian sand is exposed in the area. Because of their small thickness (1-2 m) and localized occurrence, these bodies of sand are not considered to be major hydrogeologic units. The lower part of the MA-1 unit grades downward into clay and clayey silts of the upper member of the Sehoo Formation. Sand partings become less abundant with depth. Within the unit, ground water moves almost exclusively through the alluvial sands.

Primary Aquifer 1 (PA-1)

Primary Aquifer 1 (PA-1) underlies MA-1 in the western part of the study area, but is not exposed. It reaches a maximum thickness of 6 m in the west; however, it thins to the east and eventually pinches out in the central part of the study area. The water-bearing sands are probably post-Lake Lahontan channel deposits of the Carson River. The unit also contains interbedded silt and sandy clay, probably deposited when the river channel was inundated by shallow lakes.

Confining Bed 1 (CB-1)

Confining Bed 1 (CB-1) is probably the equivalent of the lower member of the Sehoo Formation. It underlies MA-1 everywhere except in the north where it is exposed and in the west where it underlies PA-1. Thickness is highly variable, ranging from 1 to 10 m. Northern exposures are discontinuous where CB-1 is locally overlain by shallow deposits of eolian sand. The unit is essentially a deep-lake clay but has basaltic sand and volcanic ash partings which are laterally extensive. This clay probably was deposited when Lake Lahontan reached its second highest stage of 1,332 m above mean sea level. CB-1 overlies and confines Primary Aquifer 2 which is described below.

Primary Aquifer 2 (PA-2)

The boundary between CB-1 and PA-2 is sharp and seems to correlate with the contact of the Sehoo and underlying Wyemaha Formation. Primary Aquifer 2 (PA-2) was penetrated by each of the 16 test holes and is of fairly constant thickness (15 m) except in the southern part of the area where it thins to about 5 m. The unit is dominated by medium- to fine-grained black sand which yields moderate amounts of water to wells. The water is commonly under artesian pressure, and contains small amounts of natural gas derived from highly organic silt and clay within the unit. The beds of organic, black silt and clay are chiefly in the upper part of the unit and have a peaty hydrogen-sulfide odor.

Confining Bed 2 (CB-2)

Confining Bed 2 (CB-2) underlies PA-2 throughout the area and is as thick as 15 m. It thins to the south as it laps up on the northern flank of the Lahontan Mountains. Although the unit as a whole acts as a confining bed, the lithology of the unit is more variable than that of CB-1. Silty and sandy clay and stringers of sand and silty sand are abundant. Geophysical logs suggest the presence of a layer of ash of unknown origin overlying the unit throughout the area. The gamma-gamma, neutron, and natural-gamma logs indicated a layer 0.3-0.5 m thick characterized by low density, low porosity, and high gamma-ray emission at depths of between 20 and 30 m in nearly every test hole. This layer was considered a stratigraphic marker and was useful in making structural and paleotopographic inferences. Correlation with the Pleistocene Eetza Formation is considered tentative. Little is known about the contact of the Eetza and Wyemaha Formation within the basin because of the absence of exposures. The silt and clay of CB-2 lack the organic character of the Wyemaha Formation, which may indicate deep-water deposition.

Primary Aquifer 3 (PA-3)

Primary Aquifer 3 (PA-3) consists of several thin confined aquifers

separated by thin confining beds. Although the top of the unit is readily distinguishable from CB-2, the location of the bottom of the formation is uncertain, mainly because of lack of information. The unit is at least 8-10 m thick and apparently underlies CB-2 throughout the area. Water levels in wells tapping this aquifer are higher than in wells that tap either deeper or shallower aquifers. A sequence of thin beds of silt, silty clay, and sandy clay form the confining beds for the interbedded medium-grained black sand. Indivdual beds of sand and clay are of roughly equal thickness, approximately 2-4 m. PA-3 intertongues with the overlying CB-2 and underlying CB-3.

Confining Bed (CB-3)

On the basis of limited information from two test holes of 90 and 154 m in depth, Confining Bed 3 (CB-3) extends 10 to 20 m below its boundary with PA-3 before it gives way to interbedded sand and clay. The unit is composed of silty to sandy clay and some shaly clay. The beds commonly decrease in grain size downward.

Structure

The work of Morrison (1964), Stanley, Wahl, and Rosenbaum (1976), and Grannell (written communication, 1978) as well as data collected for this study, have led to the interpretation of the faults shown on plate 1. The geologic structure of the area is controlled by high-angle, northwest- to northeast-trending basin-and-range faults which range in age from pre-Miocene to Holocene. The Tertiary volcanic rocks underlying the upper sequence of sedimentary deposits are broken by at least two sets of faults (Grannell, written communication, 1978): (1) An older, northwesterly trending system of faults probably formed prior to Miocene vulcanism and, (2) younger faults of late Pliocene age which cut off the older faults as their trends change from north to northeast. According to Morison (1964) the climax of basin-and-range deformation in the

area probably began during the Pleistocene and continued to pre-Lake Lahontan late Pleistocene time. The last major episode of faulting in the Stillwater area likely occured in late Pleistocene time and resulted in numerous arcuate faults, only a few of which are exposed in the unconsolidated basin fill.

The Miocene and older faults are exposed only at Rainbow Mountain where they break the basalt of Rainbow Mountain into N. 15^{o} E. to N. 25^{o} W. trending blocks up to 3 km long. The overlying dacite of Rainbow Mountain as well as the Eagles House Ryholite and the Tertiary Truckee Formation are somewhat less faulted. A major fault of this age and orientation is concealed beneath Lake Lahontan sediments just east of Stillwater (see pl. 1.). This fault has been identified by Beuck (written communication, 1964); Olmsted, Glancy, Harrill, Rush, and Van Denburgh (1975); and Stanley, Wahl, and Rosenbaum (1976) as being the conduit that transmits goethermal fluids from the deep reservoir. Stanley, Wahl, and Rosenbaum support this interpretation by noting an aeromagnetic low coincident with the fault which may indicate that upwelling thermal water has altered magnetic minerials to nonmagnetic ones.

The northeast-trending fault system is an active one; it was identified as the locus of the two magnitude 6 Fallon earthquakes of June and August 1954. These en echelon faults can be traced for more than 30 km from near Salt Wells (on U.S. Highway 50) northward to the Stillwater Lakes. They roughly parallel the mountain-front scarp of the Stillwater Range from Salt Wells to a point east of Stillwater. North of this point, the mountain range diverges approximately 5° to the east. Grannell (written communication, 1978) postulates that the intersections of the northeast-trending fault system with the mountain-front faults and the northwest-trending faults probably form extensive crush zones within the basement rocks, giving them fracture permeability conducive to the formation of a geothermal reservoir.

The existence of many early Pleistocene faults is inferred from truncated

bedrock exposures and linear mountain-front scarps, such as at Stillwater Point approximately 7 km east of Stillwater (Morrison, 1964). The basin-interior faults of this age strike from N. 30° E. to N. 20° W., have throws of less than 30 m, and generally show little gouge and no hydrothermal alteration.

The lakes and marshes that extend north of Stillwater lie within a topographic depression which is paralleled at its margins by low ridges striking N. 20°-45° E. and having 2-5 m of relief. The orientation of the ridges and troughs diverges by approximately 60° from the trend of local deflation features. The lakes and marshes probably lie within a foundered graben bounded by faults which are associated with early Pleistocene faults upon which subsequent movement has occurred and been transmitted along zones of weakness through the overlying lake deposits.

A geothermal test well drilled in the southwest quarter of section 6, T. 19 N. R. 31 E., encountered "red, highly altered, chloritic basalt" at a depth of 914 m. (Beuck, written communication, 1964). This is probably one of the upper flows of the Pliocene and Pleistocene Bunejug Formation. The major northwest-trending fault discussed above lies just east of this location and is estimated to have displaced the Tertiary section downward 250-300 m on the east side (Bueck, written communication, 1964). This red basalt is probably at the top of a sequence of Tertiary volcanic rocks which is broken into a complex series of blocks by the intersecting northwesterly and northeasterly faults. Grannell's data (written communication, 1978) suggest that these blocks form at least three grabens which terminate near the center of the thermal anomaly and radiate outward to the northeast and east-by-northeast.

HYDROLOGY

Surface Water

Surface water is routed into the study area by a network of irrigation canals which receive outflow from Lahontan Reservoir. The main canals are the Ole's Pond Outlet, the "S" line, the "S1," and the "L" line, all of which enter the study area from the southwest. Of these, the most important is the "S" line which feeds Harmon Reservoir. Harmon Reservoir has a maximum operating capacity of 2.1 hm^3, (Glancy and Katzer, 1975). The only natural stream channel of any size in the area is the Stillwater Slough, which begins near Harmon Reservoir and meanders northeastward through Stillwater into the Wildlife Management Area. Stillwater Point Reservoir, 2 km southeast of Stillwater, has a maximum operating capacity of 8.6 hm^3, (Glancy and Katzer, 1975). However, in recent years Stillwater Point Reservoir has remained almost dry.

Five gaging stations within the study area are operated by the U.S. Geological Survey. The total flow at these stations, plus that of a sixth located immediately west of the study area, represents the outfall from the Newlands Project into the Stillwater Wildlife Management Area and the Carson Sink. Locations and available records for the stations are listed in table 2. At present, inflow to the study area is not measured. Other than precipitation, the outfall from the Newlands Project is the only source of water for the Stillwater Marsh. Since 1972 the wetland acreage has decreased steadily from nearly 65 km^2 to 14 km^2 in 1977, (U.S. Fish and Wildlife Service, 1978).

TABLE 2.-- Selected streamflow records.

USGS station no.	Station	Location no.	Total annual discharge, hm^3 (calendar year) 1967	1968	1969	1970	1971	1972	1973	1974	1975	1976	1977
10312210	Stillwater diversion canal near Fallon	19/30-34aa	44.0	35.8	44.3	77.2	54.6	40.3	33.0	32.7	42.7	26.1	11.0
10312220 1/	Stillwater slough cutoff drain near Stillwater	20/31-32cd	29.3	32.1	35.6	38.3	25.9	28.1	26.3	25.4	24.7	17.3	10.2
10312240 1/	Paiute diversion drain near Stillwater	20/30-36bc	9.19	6.47	8.90	11.8	7.95	7.83	7.94	6.65	6.60	6.10	3.94 2/
10312260	Indian Lakes canal near Fallon	20/29-26ab	22.4	12.8	20.6	20.0	22.8	19.4	11.0	14.9	17.8	12.5	5.2
10312265 3/	Indian Lakes canal below East Lake	20/30-14a	----	----	----	----	----	----	----	----	----	----	----
10312270 3/	Paiute drain at wildlife entrance near Stillwater	20/34-7cc	----	----	----	----	----	----	----	----	----	----	----

Footnotes:

1/ 1967-1974 average used to compute surface-water outflow in water budget.

2/ Estimated.

3/ Established April 1977.

Precipitation

The average annual precipitation recorded at the Fallon Experimental Station for the 72-year period from 1906 to 1977 was 128 mm/yr (from NOAA). During the period October 1970 through September 1972 a field rain gage was maintained near Stillwater as a part of a Newlands Project water study made by the College of Agriculture, University of Nevada, Reno (Guitjens and Mahannah, 1976). The total precipitation measured at Stillwater for these two years was about 30 mm/yr less than that measured at the Fallon Experimental Station. The difference is consistent with the interpretation of Hardman (1965), who showed that the Carson Sink and much of the surrounding area receives on the average less than 100 mm/yr. However, because of the much greater length of record, the average annual precipitation at Fallon was used in the computation of the water budget presented in a later section.

Evapotranspiration

Evapotranspiration (ET) includes evaporation from soil and water surfaces as well as transpiration by native vegetation and irrigated crops.

Ground cover within the area was categorized by evapotranspiration rate. For the water budget presented later in this section the area of each ground cover type within the budget area was multiplied by an estimated annual rate of evapotranspiration for that type to obtain an annual rate of discharge. By summing the products, the total annual discharge from the budget area was estimated (table 3).

The five types of ground cover defined for this study and their distribution are shown on plate 3. Type 1, lakes and wetlands, includes all areas of open water, marshes, meadows, and mudflats. Typical vegetation ranges from sago pondweed, coontail, and duckweed to cattail, hardstem bulrush, and saltgrass. The annual rate of evapotranspiration for type 1 ground cover was synthesized from estimates made for the Newlands Project area in a hydrologic study by Clyde-Criddle-Woodward (1971). Rates of evapotranspiration for various densities of phreatophytes as well as for permanent and temporary open water were weighted by the percentage of type 1 ground cover that each accounted for in the budget area. The annual rate arrived at by this method was 1.36 m/y. This compares well with the rate of 1.37 m/yr used in the Stillwater Wildlife Management Area by Green, Gallagher, and Bianchi (1975).

Type 2 ground cover includes all crops grown in the area as well as pasture, yard, and brush areas. The main crop and ground cover is the phreatophyte alfalfa. Hay and grain are the only other crops of significance in the area. Estimates of consumptive use for alfalfa in the Fallon area range from 0.71 m/yr (Clyde-Criddle-Woodward,1971) to 1.01 m/yr (Guitjens and Mahannah, 1976). The value of 1.01 m/yr is probably more accurate for the Stillwater area because this rate was derived from experiments on a 30-acre test plot within the

TABLE 3.-- Estimated average annual discharge by evapotranspiration from the hydrologic-budget area.

Groundcover type [1]	Area ($m^2 x 10^6$)	Evapotranspiration rate (m/yr) [2]	Annual discharge (hm^3)
1	23.5	1.36	32.0
2	36.1	0.87	31.4
3	21.4	0.18	3.9
4	19.5	0.12	2.3
5	none	0.09	none
Total	100.5		69.6

Footnotes:

[1] Mapped on plate 3, described in section on "Evapotranspiration.

[2] From table 4.

area. Annual consumptive use for pasture acreage is 0.85 m/yr and for grain is 0.49 m/yr, as computed by the Soil Conservation Service for the Fallon area.

Discharge by type 2 ground cover within the water budget area was computed using an estimated annual rate of evapotranspiration of 0.87 m/yr. This rate was determined by Green, Gallagher, and Bianchi (1976) to represent the average consumptive use on the Newlands Project for crops listed in the 1974 crop census.

Ground-cover types 3 and 4 are dominated by species known as salt-desert shrubs. The most important of these shrubs are big greasewood, dryland greasewood, four-wing saltbrush, and shadscale. The most common grass is saltgrass; however, Indian rice-grass and squirrel-tail can also be found. Types 3 and 4 are differentiated on the basis of density of vegetation rather than on type of vegetation, although relative percentages of the various types vary areally. No definitions for the terms "dense" and "sparse" were ever assigned during the mapping procedure; however, a typical dense stand of greasewood contained approximately 3-4 shrubs per 10 m^2. Anything less was considered sparse.

Olmsted, Glancy, Harrill, Rush, and Van Denburgh (1975) used evapotranspiration rates ranging from 0.25 m/yr for dense saltgrass with or without greasewood to 0.03 m/yr for sparse greasewood. Clyde-Criddle-Woodward (1971) suggested rates of 0.86-1.22 m/yr for densities from "light" to "heavy". To add to the diversity of estimates, Robinson (1958) assigned a rate of 0.66 m/yr for dense stands of greasewood where the depth to the water table is 0.5 m.
The main difficulty in assigning evapotranspiration rates to ground cover types 3 and 4 was interpreting the subjective terms for density of vegetation used in the above references and relating these to the densities existing in areas mapped as type 3 or type 4. Extensive water-budget studies by the U.S. Geological

Survey in the high desert areas of northern and central Nevada tend to support the range of values given in Olmsted, Glancy, Harrill, Rush and Van Denburgh (1975) (Glancy, oral communication, May 1978). The evapotranspiration rate assigned to type 3 was that for "dense to scattered saltgrass with greasewood and or rabbitbrush," 0.18 m/yr. The sparsely vegetated rangeland, type 4, was estimated to evapotranspire 0.12 m/yr.

Barren-land and playa deposits are mapped as type 5 ground cover on plate 3. The estimated rate of evaporation from playas of 0.09 m/yr used by Olmsted, Glancy, Harrill, Rush, and Van Denburgh (1975) is based in part on studies by M. L. Sorey (written communication, 1971) at Smith Creek Playa in central Nevada. Sorey derived this estimate from the degree of curvature of the temperature profile, which is dependent on the rate of vertical ground-water flow. The many variables influencing rates of evaporation from playas, such as depth to water table, temperature and properties of near-surface materials, make Sorey's estimate very site-specific. However, for this study, barren land and playa deposits do not cover a significant portion of the water budget area and so are not used in the calculation of total evapotranspiration. The rate is included for informational purposes only.

Estimated rates of evapotranspiration for the five ground-cover types are summarized in table 4.

TABLE 4. -- Estimate annual rates of evapotranspiration for ground water types within the Stillwater geothermal area.

Groundcover type	Description [1/]	Annual evapotranspiration, m
1	Lakes and wetlands	1.36
2	Agriculture areas	0.87
3	Densely vegetated rangeland	0.18
4	Sparsely vegetated rangeland	0.12
5	Barren areas, playa deposits	0.09

[1/] See text for complete description.

Movement and Occurrence of Shallow Ground Water

For descriptive purposes, the shallow ground-water flow system is defined as consisting of lacustrine and subaerial deposits of Lake Lahontan and post-Lake Lahontan age. From the few deep well logs available, the thickness of these deposits is estimated to be approximately 300 m near Stillwater, probably thinning to less than 200 m at the eastern margin of the study area. Thickness almost certainly increases basinward; however maximum thickness is unknown. The hydraulic relationship between the interbedded silt, sand, and clay, of Pleistocene Lake Lahontan and the underlying calcareous sandstone and shale of Tertiary age is poorly understood. A basic change in geohydrologic character is likely, which is the rationale for placing the lower boundary of the shallow ground-water system at the base of the Lake Lahontan deposits.

The complex series of intertonguing sands and clays found in the upper few tens of meters is probably characteristic of the system throughout the thickness. As in the upper part of the section, continuous sand aquifers are probably rare. The major volume of lateral ground-water movement occurs through "aquifer zones" where tongues of sand are dominant and are hydraulically interconnected, in spite of abundant clay interbeds. Water-table conditions exist to a depth of 5-10 m at most places, below which confined conditions prevail.

Depth to the water table in April of 1978 ranged from 1 to 4.5 m within the study area. Heads measured in confined zones between 14 and 152 m ranged from 5.7 m below to 3.6 m above land surface. Annual fluctuations in the water table rarely exceed 2 m. Highest water levels occur in middle to late spring, then drop off rapidly in June or July and reach a minimum by September. A hydrograph for a shallow piezometer (OB-2A) is shown in figure 3. This piezometer is just north of the irrigated area (pl. 3). Small peaks in the hydrograph represent irrigation applications. Beginning in water year 1978 (October 1, 1977 - September 30, 1978) water levels were down an average of 0.50 m from levels

FIGURE 3. -- Water level changes in observation well OF-2A

for the same time in 1977 for this particular piezometer. Lower water levels were caused by the reduced water receipts of local farmers and the resulting stress put on the ground-water system by an increase in subirrigation by alfalfa (Green and others, 1976). Long-term water-level data for the confined system are not available. Annual fluctuations probably are less than for the shallow system, and as depth increases, response to irrigation applications probably is attenuated.

The generalized surface of the water table (fig. 4) is a muted replica of the topographic trough extending northeastward through the area. Figure 5 shows the potentiometric surface plotted from data from test holes that penetrate primary aquifer 2 (See section, "Hydrogeologic Units," for description.) Most of the canals and drains of the Newlands Project lie southwest of Stillwater and their importance as a source of recharge to primary aquifer 2 is reflected in the rise in the potentiometric surface in that direction. The configuration of the potentiometric surface constructed using data from test holes penetrating primary aquifer 3 is shown in figure 6. This surface bears a striking contrast to that of primary aquifer 2. Streamlines superimposed on this diagram indicate two general directions of ground-water movement. An influx from the southwest is evident in primary aquifer 2, but there is also apparent lateral ground-water inflow from the south. This indicates a hydraulic connection between the sands of primary aquifer 3 and recharge areas in the uplands near Rainbow Mountain. To confirm this interpretation, much more water-level data would be necessary as the equipotential lines are based on few data points.

Two factors that may affect heads measured in the area are structural compartmentalization by faulting and thermo-artesian conditions caused by thermal convection in response to the lower density of hot water. Although a number of recent faults transect the near-surface deposits, compartmentalization

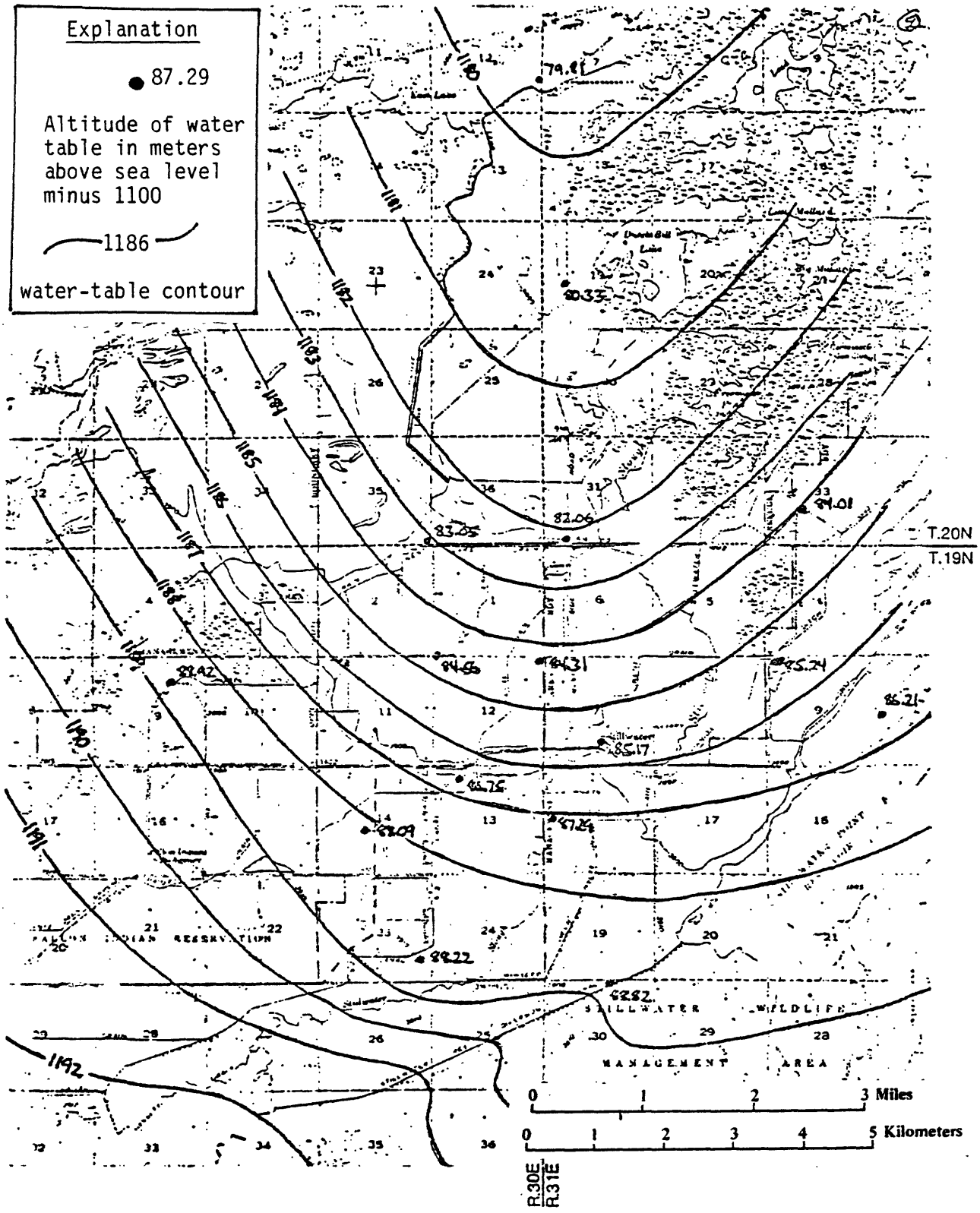

FIGURE 4. -- Altitude of water table, April 1978

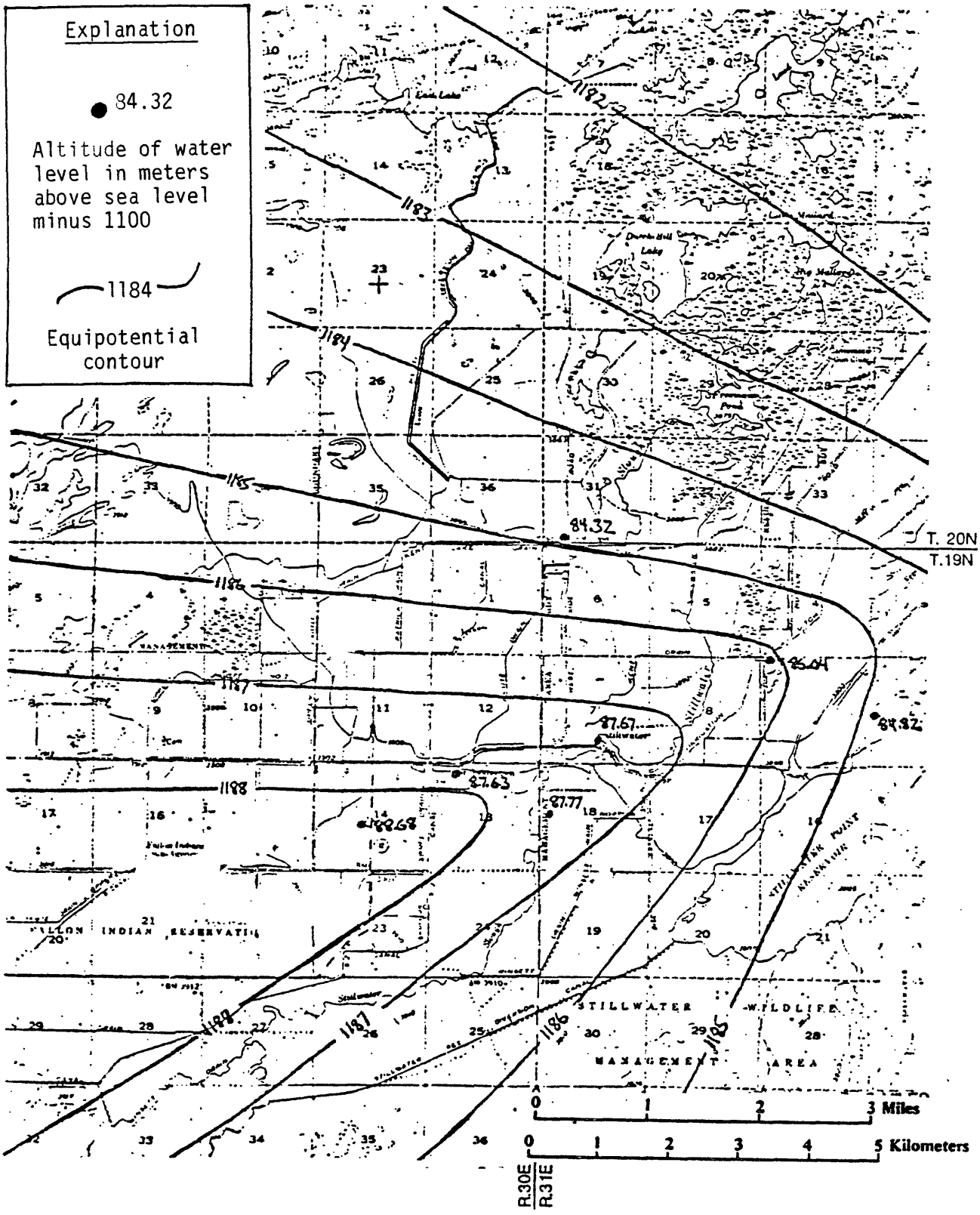

FIGURE 5.-- Altitude of confined potentiometric surface, primary aquifer 2, April 1978.

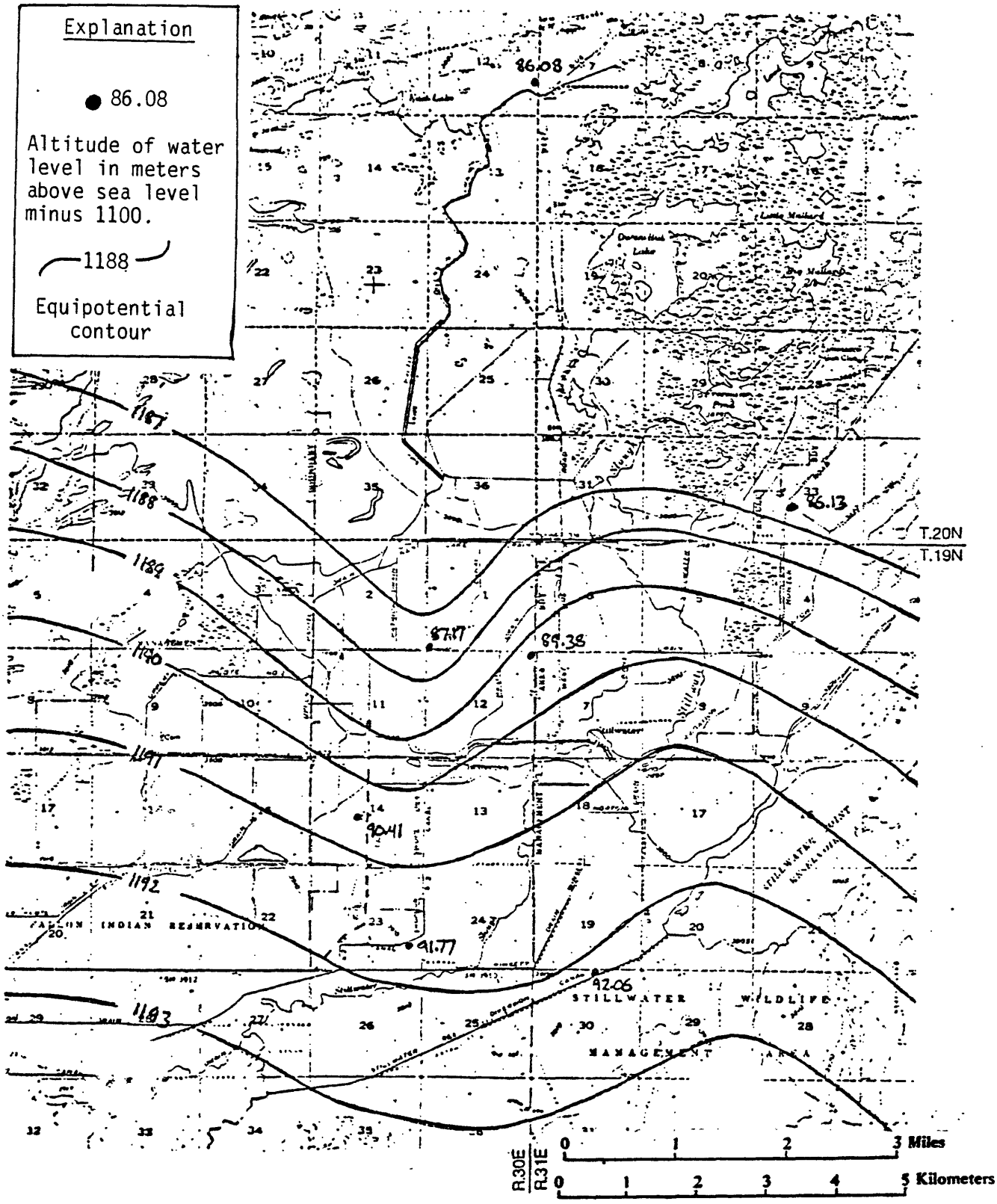

FIGURE 6.-- Altitude of confined potentiometric surface, primary aquifer 3, April 1978.

is not indicated by the data.

The influence of thermo-artesian conditions on water levels was tested by correcting the measured head in test hole CDDH-117A for thermal-density effects. This test hole in the village of Stillwater had the highest temperature gradient of any of the test holes (nearly 3,600°C/km). The column of water in the pipe was divided into intervals of 1-8 m in length and a mean temperature was assigned to each interval. The equivalent head in an isothermal column of water at a temeperaure of 18°C was computed using the relationship

$$h_{18^o} = \frac{\gamma i}{\gamma 18^o} hi_{Hot}$$

where h is the head, γ is the specific gravity of water at the average temperature for the interval, and i indicates the interval. For each interval the specific gravity of water at the mean temperature of that interval was used to convert the length of that interval, h_i, to an interval of length h_{18^o}. The values of h_{18^o} for each interval were summed to obtain the head in CDDH-117A corrected for thermo-artesian effects. For a column of water 19.78 m in length ranging in temperature from approximately 18°C at the top to about 65°C at the bottom, the temperature-density effect was found to increase the head by 0.17 m. Considering that the temperature gradients in most of the other test holes were at least an order of magnitude less than that in CDDH-117A, it was determined that thermo-artesian effects could be ignored for the purpose of constructing potentiometric-surface maps. This does not introduce significant error compared to the uncertainty in the land-surface altitudes, which are accurate to $\pm$ 0.25 m.

Altitude of confined water levels seems to increase with depth. Only one of the test holes that penetrate primary aquifer 2 has a water level above land surface, whereas, of those test wells penetrating primary aquifer 3, only one has a water level <u>not</u> above land surface. The two deepest test holes, CDDH-106C (92.7 m) and

CDDH-102A (152.8 m) flow only slightly. Artesian heads generally increase toward the north with decreasing altitude of land surface. Flow-rates of the test holes are highly variable, owing in part to the completion method used in each hole and the level of development attained with airlift pumping. The observed maximum was 0.76 L/min, and the minimum was a slow trickle of less than 0.008 L/min.

Vertical hydraulic gradients were computed at each test-hole site. These values are plotted on plate 3. Upward gradients exist at every site except for CDDH-111A, which indicates net ground-water discharge. Test hole CDDH-111A is in a barren area, and is the test hole closest to the alluvial fans of the Stillwater Range. The downward hydraulic gradient at this location probably is the net result of recharge from the adjacent alluvial apron, a low rate of discharge by evaporation from the unvegetated playa soil, and a relatively great depth to water. The only apparent areal trend in vertical hydraulic gradient is a north-northwesterly lineation of high positive (upward) gradients. This feature is probably related to fault-controlled upflow of thermal water. At site CDDH-106, variation of vertical hydraulic gradient with depth was analyzed. Gradients for the three test holes here of depths 17.70, 51.50, and 92.70 m were +0.04, +0.05, and +0.03, respectively. Within error of the measurement, vertical hydraulic gradient appears to be constant with depth. Lateral potential gradients are much less than the vertical gradients in the area. Average lateral gradient within the unconfined zone is 9.6×10^{-4}. Within the confined aquifers, average gradients are 6.7×10^{-4} in primary aquifer 2, and 7.6×10^{-4} in primary aquifer 3.

Despite the fact that vertical potential gradients are much greater than lateral gradients, lateral flow velocities exceed vertical flow velocities throughout the study area. Confining beds of clay and silt have extremely low vertical hydraulic conductivities and the large vertical potential gradients

are in these beds rather than in the aquifers. The calculated vertical gradient is the mean of very high gradients through the confining beds and very low gradients through the sand aquifers.

The large upward vertical potential gradients indicate that a large volume of ground water is drawn up through the roots of plants and discharged as evapotranspiration. The remainder of discharge moves north-northeastward to the Carson Sink as lateral subsurface outflow until it is discharged by evaporation from the barren playa. The shallow ground-water system is recharged by infiltrated irrigation water, lateral ground-water influx, precipitation on the adjacent mountains and upland slopes, and upflowing thermal ground water. The relative importance of each will be discussed in the following section; however, infiltrated irrigation water is the major contributor.

Water Budget

A water budget was computed for the area of 100.5 km^2 enclosed by the 3 hfu isogram shown on plate 3. The purpose of the budget was to estimate the rate of discharge of thermal ground water upward into the shallow aquifers. In addition, a better picture of the overall hydrologic system was gained by quantifying the gross inputs and outputs. Figure 7 shows a sketch of the vertical and lateral boundaries of the budget volume as well as the modes of inflow for which estimates were made. To compute the budget the following assumptions were made:

1. All surface-water inflow was assumed to enter the area through canals and laterals as farm irrigation receipts. Total surface-water inflow was computed by taking the irrigated acreage of the budget area plus the area within the Canvasback Gun Club (see pl. 1) having water-rights and factoring this sum by the estimated 1.52 m depth of water diverted annually to the Newlands Project area. (Clyde-Criddle-Woodward, 1971).
2. In computing lateral ground-water inflow and outflow, an average hydraulic conductivity of 12.2 m/day (300 gpd/ft^2) was assumed on the basis of laboratory measurements performed on similar materials from the Carson Sink. (Irwin Remson, written communication, 1978).
3. The lower boundary of the budget volume coincides with the lower boundary of primary aquifer 3. All lateral ground-water movement is assumed to occur within marginal aquifer 1 and primary aquifers 2 and 3. Average saturated thickness, widths of flow section, and potential gradients were estimated from plate 3 and figures 4 and 5; these are listed in table 5.
4. Precipitation within the budget area is assumed to be uniform and equal to that measured at the Fallon Experiment Station.

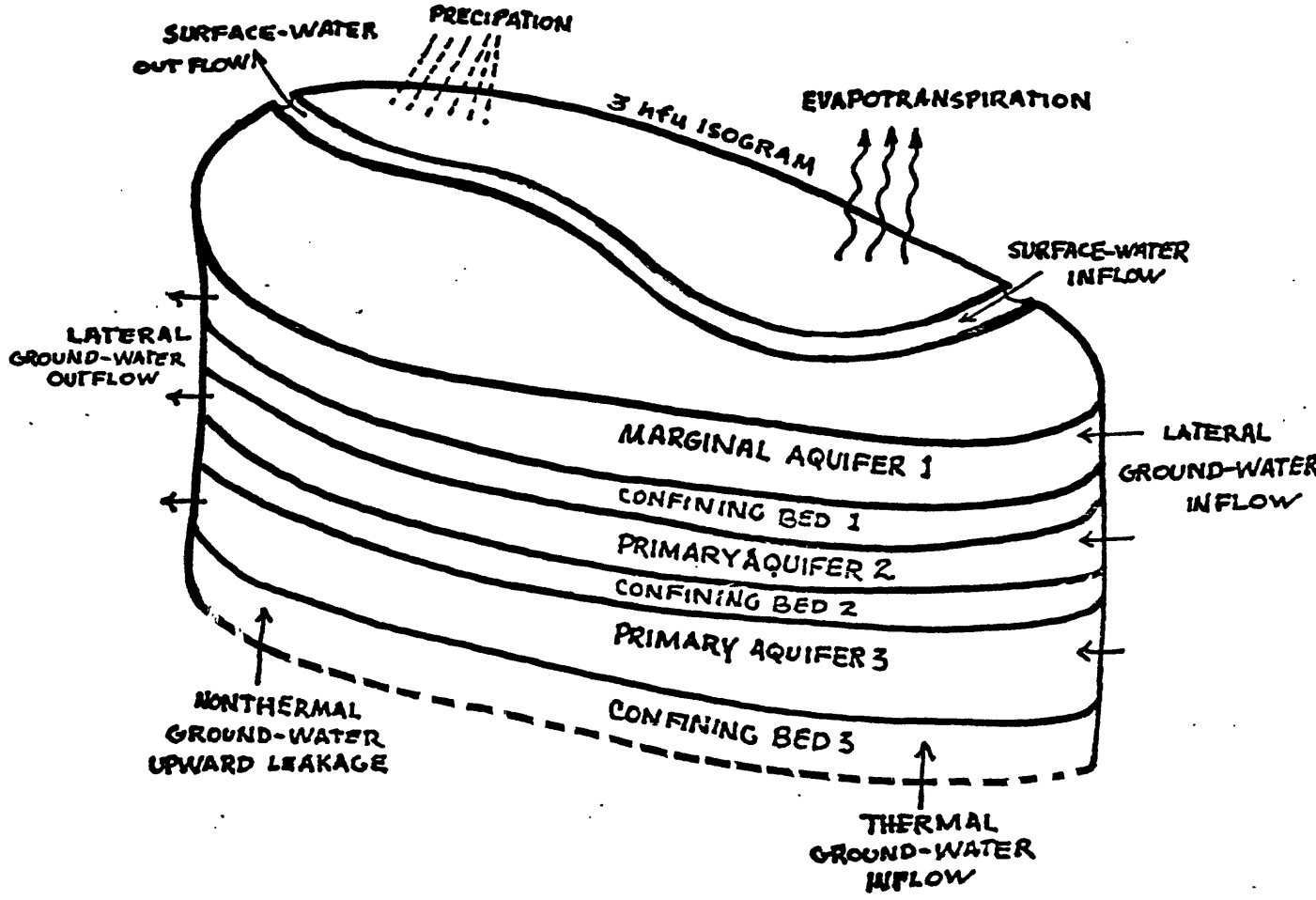

FIGURE 7. -- Generalized sketch of hydrologic budget volume showing inputs and outputs for which estimates were made

TABLE 5. -- Estimated average saturated thickness, potential gradient, and width of flow section for the hydrologic budget area [1/]

INFLOW	Marginal aquifer 1	Primary [2/] aquifer 1	Primary aquifer 2	Primary aquifer 3
Potential gradient ($\times 10^{-4}$)	9.6	8.5	7.5	9.4
Saturated thickness m	10	10	15	10
Width of flow section ($m \times 10^4$)	3.6	---	1.1	2.2
TOTAL INFLOW ($m^3 \times 10^6$/yr)	1.53	---	0.55	0.91
OUTFLOW				
potential gradient ($\times 10^{-4}$)	6.5	6.0	5.6	11.7
Saturated thickness m	10	10	15	10
Width of flow section ($m \times 10^4$)	0.5	---	3.0	1.9
TOTAL OUTFLOW ($m^3 \times 10^6$/yr)	0.15	---	1.13	0.99

Footnotes:

[1/] Width of flow section is measured along the circumference of the 3 hfu isogram shown in plate 3.

[2/] Primary aquifer 1 is discontinuous beneath the study area, values listed are "best estimates" from available data.

5. Surface-water outflow is assumed to be equal to the average total discharge measured by the gages indicated in table 4 for the period 1967-74.

6. Upward leakage of nonthermal ground water is assumed. It is estimated to occur throughout the area under an upward gradient of 0.04 across a fairly impermeable boundary having an average vertical hydraulic conductivity of 0.1 m/day.

The water budget which was computed based on the assumptions above is presented in table 6. If the estimated inflows and outflows were accurate and all water passing in and out of the budget volume were represented by these estimates, then the residual, 22 hm^3/yr, could be wholly attributed to thermal ground water entering the budget volume from depth. Realistically, the error associated with the estimate of either of the two largest items (surface inflow, or evapotranspiration) could account for the residual. The nature of the study area, with large volumes of irrigation waters passing through it, infiltrating, and evapotranspiring, is not conducive to solving for an unknown like thermal ground-water upflow which may be less than 2 percent of any one of the major budget items.

In a following section, "Temperature distribution and heat flow", discharge of thermal ground water is estimated by the heat-budget method. Annual discharge of thermal ground water by this method equals approximately 1.6 hm^3/yr. This method, the assumptions made, and relative error will be discussed in the next section; however, the number of unknowns and errors introduced by each are less than those incurred in the water budget computation. In light of this, perhaps a more accurate water budget would result if the most difficult item to estimate, surface-water inflow, were considered the unknown. Thus, balancing the budget with an estimated thermal ground-water

TABLE 6.-- Water budget for the hydrologic-budget area.

INFLOW	Annual volume (hm^3)
Surface water	72.0
Lateral ground water	3.0
Precipitation	12.8
Nonthermal upward leakage	0.1
TOTAL INFLOW	88 (rounded)
OUTFLOW	
Surface water	38.5
Lateral ground water	2.2
Evapotranspiration [1/]	69.6
TOTAL OUTFLOW	110 (rounded)
RESIDUAL (= total inflow - total outflow)	-22

Footnote:

[1/] See table 3 for derivation of estimate.

influx of 2 hm^3/yr would yield a rate of 92 hm^3/yr attributable to surface-water inflow. This is about 22 percent more than the original estimate and is probably more accurate.

Lateral ground-water movement and upward leakage of nonthermal ground water were also difficult to estimate owing to lack of information on the hydraulic properties of the flow media. However, because of their relatively small magnitude, large errors in their estimation do not cause large errors in the total budget. This budget might be refined in the future by using the discharge measured at the two stations listed in table 2 that were established in 1977 to estimate surface-water outflow from the area.

Ground-Water Quality

General Chemical Characteristics

The dissolved-solids concentration of shallow ground water in the Stillwater area decreases with depth. The water of the shallow, unconfined system is of poor quality with dissolved-solids concentration averaging more than 16,000 mg/L. Water from deeper (> 10 m) aquifers generally is of better quality, but dissolved-solids concentration still averages more than 6,000 mg/L. In contrast with most thermal-nonthermal ground water systems, the most dilute ground water in the area is thermally derived or mixed with thermal water. Water of this type sampled in the area ranges in temperature from 47^{o} to 96^{o}C and has an average dissolved-solids concentration of about 4,000 mg/L. The eighteen chemical analyses shown in table 7 were categorized on the basis of depth and temperature, as follows: (1) Deep thermal ground water and mixtures of thermal water and nonthermal ground water having a temperature greater than 47^{o}C; (2) nonthermal ground water from a depth of at least 17 m having a temperature of less than 47^{o}C; (3) shallow ground water from the unconfined zone; and (4) inflowing surface irrigation water. For each category, the average chemical make-up and the range of values of each constituent are given in table 8.

Being an agricultural area in a closed desert basin, the Stillwater area requires a large proportion of irrigation water solely for the leaching of excess salts from the soil. During 1976-78 farmers received as little as 50 percent of their water-right because of drought. This caused considerable salt build-up as evidenced by chemical analyses of water from the shallow ground-water system. The extent of salt build-up is especially striking when the salt content of incoming irrigation water is compared to that which has infiltrated to the water table. The ratio of dissolved-solids concentration in the shallow ground water to that in the irrigation water is approximately 40:1.

TABLE 7. -- Chemical analyses [1] and selected ratios for wells and test holes.

Ground water category	Well number	Location number	Date sampled	Depth to screen m	Temp. °C	pH	Spec. cond. Mmhos/s	Concentration of dissolved constituents, mg/L														Ratios of milli-equivalents except where noted ionic ratios						
								SiO_2	Ca	Mg	Na	K	As	B	Li	Rb	HCO_3	CO_3	Cl	F	SO_4	Cl/F	Cl / (HCO_3+CO_3)	Ca/Mg	Na/Ca	Na/K	Mg/F	SiO_2 (wt.) / B	HCO_3 / F
Deep thermal	DH-117A	19/31?dcb1	78 04 19	19.7	66.6	8.4	7480	80	71	1.1	1600	57	0.006	17	2.0	0.08	120	15	2300	3.3	180	380	26	39	20	48	0.5	4.7	11
Deep thermal	DH-123A	19/30-aaa1	78 04 23	37.1	46.4	7.6	7210	58	45	7.7	1500	25	0.003	16	1.5	0.03	310	<1	2200	1.5	4.6	790	12	3.8	29	102	7.5	3.6	64
Deep thermal	PW-44A	19/30-6bcb1	78 04 21	56.7	94.0	8.3	7570	120	75	0.9	1700	48	0.045	17	2.1	0.21	140	<1	2400	5.5	210	230	29	50	20	60	0.3	7.1	7.9
Deep thermal [2]	PW-26A	19/31-7dcc1	73 05 02	70.1	95.7	7.6	6910	170	108	1.7	1480	42	0.002	15	1.9	0.22	90	<1	2200	5.0	190	240	42	39	12	60	0.5	11	5.6
Non-thermal	DH-101A	20/30-12dcd1	78 04 20	30.6	16.9	8.2	8870	39	4.6	4.4	1900	35	0.005	25	0.09	0.02	830	71	2560	2.0	9.9	710	4.9	0.6	360	92	4.0	1.6	140
Non-thermal	DH-108A	19/31-30abb1	78 01 21	26.1	17.4	7.8	8380	58	30	11	1900	70	0.005	21	2.0	0.07	270	1	2600	2.3	210	600	16	1.7	55	46	7.4	7.8	36
Non-thermal	DH-111A	19/31-10cbb1	78 04 20	15.2	16.7	8.2	>13000	31	49	19	3000	110	0.013	20	0.31	0.02	420	3	4500	1.6	140	1490	18	1.5	54	47	16	1.6	87
Non-thermal	DH-106A	19/30-14caa1	78 01 20	17.7	15.5	8.3	>14000	33	32	47	2900	86	0.018	26	0.38	0.03	1510	54	4200	1.3	16	1720	4.5	0.4	79	57	56	1.0	360
Non- [3] thermal	AH-15A	19/30-10cdd1	73 06 28	45.2	18.5	---	>11000	27	19	25	2400	47	0.094	19	0.15	----	616	<1	3600	1.4	26	1320	10	0.5	110	87	28	1.1	140
Non- [3] thermal	AH-23A	19/30-25dbb1	73 06 28	39.1	19.0	---	7960	43	24	6.2	1700	44	0.004	22	1.1	----	276	19	2300	0.9	220	1370	13	2.4	62	65	11	2.0	110
Non- [3] thermal	AH-24A	19/31-20bbd1	73 06 28	45.4	20.0	---	7960	55	21	4.6	1700	55	0.005	21	1.7	----	241	22	2400	1.5	110	860	15	2.8	70	52	4.8	1.5	59
Shallow	AH-102B	20/31-19cbd2	78 04 22	1.7	----	7.2	>1700	2.7	960	530	2900	160	0.60	18	3.0	----	730	<1	4900	0.3	3200	8640	12	1.1	2.6	31	2724	0.2	750
Shallow	AH-106B	19/30-14caa4	78 04 22	4.0	----	7.2	>26000	38	600	1100	4400	160	0.90	18	1.3	----	570	<1	7500	1.1	4800	3650	23	0.3	6.4	47	1560	2.1	150
Shallow	AH-108B	19/31-30abb2	78 04 19	3.1	----	7.7	>28000	28	86	85	7300	210	0.70	76	3.9	----	790	<1	8700	3.8	2760	1220	19	0.6	74	59	35	0.4	64
Shallow	AH-110B	19/31-9bbb2	78 04 20	4.0	----	7.5	3420	32	14	7.7	730	21	1.60	5.7	0.24	----	580	<1	530	6.1	460	50	1.6	1.1	45	59	2.0	5.6	30
Shallow	AH-117B	19/31-7dcb2	78 04 19	3.6	----	7.0	1110	50	110	24	120	10	0.028	1.1	0.11	----	480	<1	82	0.6	110	70	0.3	2.8	1.0	20	62	45	250
Shallow	AH-123B	19/30-12aaa2	78 04 22	3.6	----	7.3	>16000	45	140	230	3700	59	0.40	22	1.2	----	320	<1	4500	1.5	2700	1610	18	0.4	23	107	239	2.0	87
Surface	S-Z canal	19/30-23aaa	78 04 22	---	12.0	7.3	540	12	29	9.2	68	5.5	0.017	0.65	0.07	20.02	160	<1	35	0.5	75	40	0.4	1.9	2.0	21	28	18	97

Footnotes:

[1] Analysis by Central Water Quality Laboratory, U.S. Geological Survey, unless otherwise noted.

[2] Analysis from Mariner and others (1974).

[3] Analysis from U.S. Geological Survey, unpublished data.

TABLE 8.-- Average concentrations of dissolved constituents in deep thermal, nonthermal, shallow ground waters, and surface water near Stillwater. All concentrations in mg/L except pH and specific conductance.

Constituent	Ground water categories: Deep thermal [1/] range	avg.	Nonthermal [2/] range	avg.	Shallow [3/] range	avg.	Surface [4/] water	Quality critera [5/]
As	0.002-.045	0.014	0.004-.094	0.021	0.4-.9	0.7	0.017	0.05
HCO_3	90-310	170	240-1,510	600	420-790	630	160	----
B	15-17	16	19-26	22	18-76	34	0.7	----
Ca	45-108	75	5-49	26	86-960	450	29	----
CO_3	0-15	4	1-54	17	0	0	0	----
Cl	2,200-2,400	2,300	2,300-4,500	3,170	4,500-7,500	6,400	35	250
F	1.5-5.5	3.8	0.9-2.3	1.6	0.3-3.8	1.7	0.5	1.5
Li	1.5-2.1	1.9	0.1-2.0	0.8	1.2-3.9	2.4	0.07	----
Mg	0.9-7.2	2.7	4.4-47	16.7	85-1,100	490	9.2	125
pH	7.6-8.4	8.0	7.8-8.3	8.1	7.2-7.7	7.4	7.3	6.5-8.5
K	25-57	43	35-110	64	59-210	150	5.5	----
SiO_2	58-170	107	27-58	37	3-45	28	12	----
Na	1,480-1,700	1,570	1,700-3,000	2,210	2,900-7,300	4,580	68	----
SO_4	5-210	150	9.9-220	100	2,700-4,800	3,350	75	250
Rb	0.03-.22	0.14	0.02-.07	0.04	----	----	<0.02	----
Specific cond. ohms/cm	6,910-7,510	7,280	7,950-14,600	10,400	17,000-28,500	23,400	541	----
Dissolved solids	----	4,430	----	6,270	----	16,100	395	500

Footnotes:

1/ Averages of CDDH's 117 and 124A, PW's 26A and 44A.

2/ Averages CDDH's 101A, 108A, 106A, 111A and AH's 15A, 23A, 24A

3/ Averages of CDAH's 102B, 106D, 108B, 117B, and 123B.

4/ From anlysis of S-2 canal

5/ From U.S. Environmental Protection Agency Interium Primary Standards.

In all three ground-water categories the dominant cation is sodium and the dominent anion is chloride; in addition, the atomic ratio of Na/Cl averages 0.7 for each category. In terms of the proportions between major ions, the mixed or unmixed deep thermal ground water and the nonthermal ground water differ little. The thermal ground water contains slightly more calcium and sulfate, whereas the deep nonthermal ground water has more sodium and bicarbonate. These differences are minor, however, and all these ground waters are classified as sodium chloride (Buck, 1966). The waters range in pH from slightly (7.4) to moderately (8.4) alkaline. The shallow ground water shows considerable diversity in chemical composition. A possible areal trend in the composition of the shallow ground water is the increase in calcium and magnesium toward the north. The solubilities of calcium and magnesium are dependent upon the availability of CO_2; and the reduction of organic matter in the swampy wetlands of the north probably supplies the additional CO_2 necessary for the increased Ca and Mg concentrations. Another product of this bacterial reduction, hydrogen sulfide (H_2S) gas, is oxidized to produce sulfate, which is also more prevalent in shallow ground water of the northern study area.

The quality of irrigation water sampled in April of 1978 was excellent, far exceeding the drinking-water standards of the U.S. Environmental Protection Agency. The only ground water sampled in the area that even approaches this quality was taken from water-table piezometers (CDAH-117B and CDAH 110B) adjacent to main irrigation canals. These samples no doubt represent dilutions of the highly saline surrounding ground water by infiltrated canal water, and the analyses were not used to compute the average composition of the shallow ground water shown in table 8. No discernible evidence indicates that areal variation in shallow ground-water composition is related to zones of thermal mixing with ground water from deep sources.

Because the dissolved-solids concentration of the shallow ground water is not less than that of the upflowing thermal ground water, many of the ionic ratios commonly used to differentiate thermal and nonthermal ground water are useless (see table 7). For example, Mariner, Rapp, Wiley, and Presser (1974) cite ratios of sodium to calcium and chloride to fluoride as qualitative geochemical indicators of thermal-aquifer temperatures; high ratios indicating highest subsurface temperatures. The high concentrations of sodium and chloride in the shallow ground water near Stillwater cause an inverse relationship for these ionic ratios as geothermal indicators, that is, lower ratios indicate higher ground-water temperature.

Ratios of chloride to total carbonate are slightly higher in the thermal ground waters than in the nonthermal ground water. This is because total carbonate concentrations decrease with temperature faster than the chloride concentrations decrease with depth. This may suggest that the thermal ground water is nearly saturated with respect to calcite and that the decrease in bicarbonate is due to a lower equilibrium constant for calcite at elevated temperature. Differences in the ratio of calcium to magnesium between thermal and nonthermal ground water are large. Thermal-water Ca/Mg ratios are on the order of 45, whereas nonthermal ratios are never greater than 3. Finally, sodium and potassium both increase with decreasing temperature and depth such that the rato of Na/K spans a range of 21-102 for all categories of ground water.

In the Stillwater area, the near-surface evaporites and clays are constantly being leached of soluble ions by large influxes of irrigation water. The highly saline ground water (leachate) migrates downward and laterally. In the deeper, confined zones, nonthermal ground water moves toward the northeast through the area, mixing locally with thermal ground water moving upward along fault-controlled conduits. The degree to which the water from the unconfined zone mixes with the confined

ground water is unknown. These conditions combine to reverse the conventional relationships between major ions in thermal and nonthermal ground water, as evidenced by some of the ratios discussed above. Under these circumstances, ratios involving some of the minor ions might prove more appropriate in distinguishing thermal and mixed waters. The ratios included in this analysis include Mg/F, SiO_2/B, and HCO_3/F.

For the three hottest waters, the Mg/F ratios are highly consistent (0.3-0.5) and are easily distinguished from those for cooler waters, which are never less than 1. The water from test hole CDDH-123A is much higher in magnesium and lower in fluoride than the other deep thermal waters; its high Mg/F ratio as well as the ratios discussed below indicates a higher proportion of cold meteoric water than the other ground waters classified as "deep thermal".

High SiO_2/B ratios were found to reflect high subsurface temperature. For the waters hotter than 47°C, the relation between temperature and SiO_2/B is approximately linear; however, more data points are necessary to verify this relation. Boron, whose concentration is controlled by the available supply in the adjacent rocks, is normally more abundant in hot ground water than in the surrounding cooler ground water. Although the boron concentration of the thermally associated waters is high (15-17 mg/L) compared with normal ground water (0.01-1.0 mg/L) the boron concentration of the shallow ground water has been increased by high evapotranspiration rates and reaches concentrations of up to 76 mg/L (CDAH-108B). The high boron can cause severe crop damage where the water table encroaches upon the root zone. Even the deeply rooted alfalfa plant, which is the main crop in the area, can tolerate only about 10 mg/L of boron where drainage is good (Green and others, 1976).

In the Stillwater area, the HCO_3/F ratio seems to be the most reliable indicator of high subsurface temperature and it is also useful for estimating the degree of mixing of thermal and nonthermal ground water. Excluding CDDH-123A, HCO_3/F

ratios decrease with temperature from 11 to 5.6 for deep thermal ground water. The ratios for the nonthermal and shallow ground water vary considerably but none are less than 30 and the average is 168.

Sodium bicarbonate is another highly soluble compound which is concentrated in desert soils by evaporation. This provides the source for large quantities of dissolved bicarbonate in the nonthermal ground water. The solubility of carbonates decreases with temperature, and if the thermal ground water is near saturation, low concentrations will result. Fluoride is readily leached from rhyolite at high temperature. These conditions combine to yield the gross differences in the HCO_3/F ratios of thermal and nonthermal ground waters.

Trace and minor elements such as rubidium and arsenic commonly have concentrations barely within the range of detection so the minor variations are difficult to interpret. Arsenic concentrations are extremely variable within each of the three ground water categories, ranging from 0.002 to 1.60 mg/L. The shallow, unconfined ground water has an average arsenic content of 0.65 mg/L (13 times that recommended for safe drinking water). Although high arsenic content is associated with thermal waters, the deep thermal water of the Stillwater area is not high in arsenic.

Rubidium was found to be a reliable indicator of high temperature. In water from the hottest wells and test holes rubidium concentrations ranged from less than 0.08 to 0.22 mg/L. No measurements were made for shallow ground water, but nonthermal water contained rubidium in concentrations ranging from less than 0.02 to 0.07 mg/L.

Mixing-Model Calculations

One objective of this study was to determine the mode and degree of mixing of cold, meteoric ground water with deep thermal ground water. Fournier and Truesdell (1974) proposed a method of using silica concentrations in water to

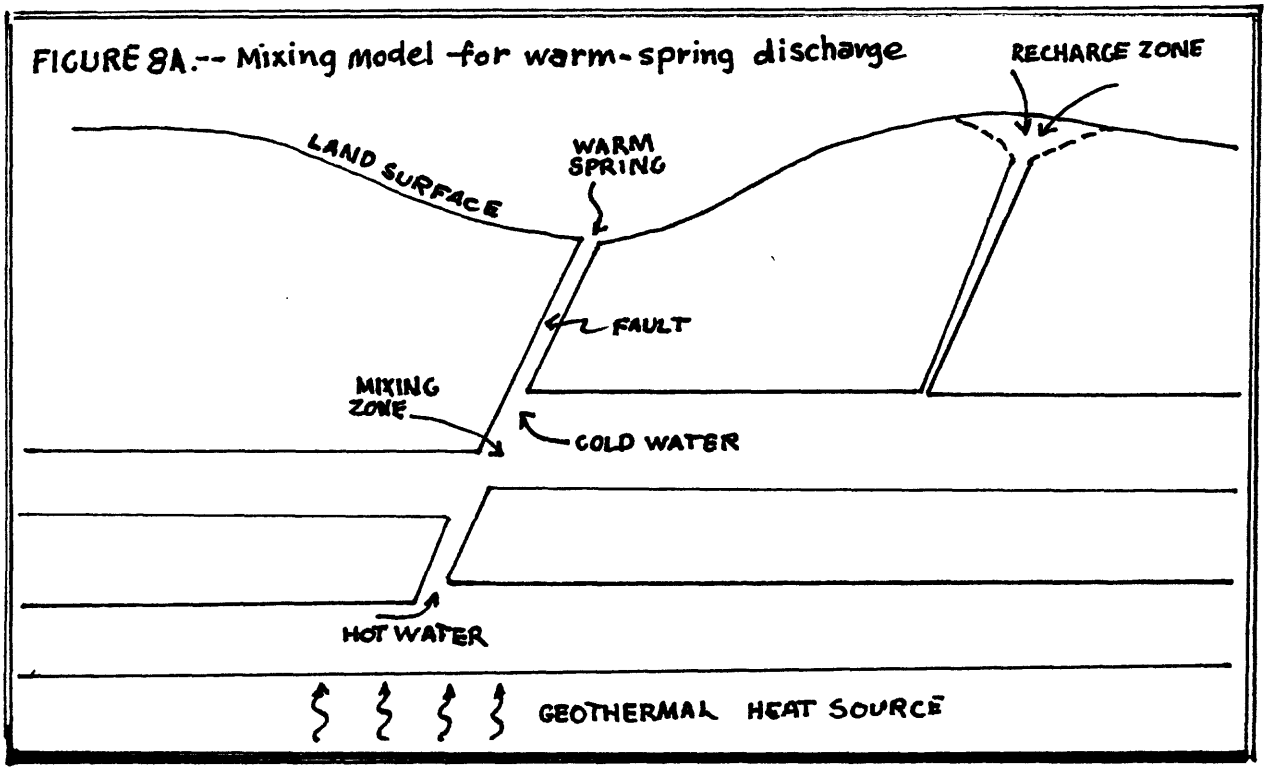

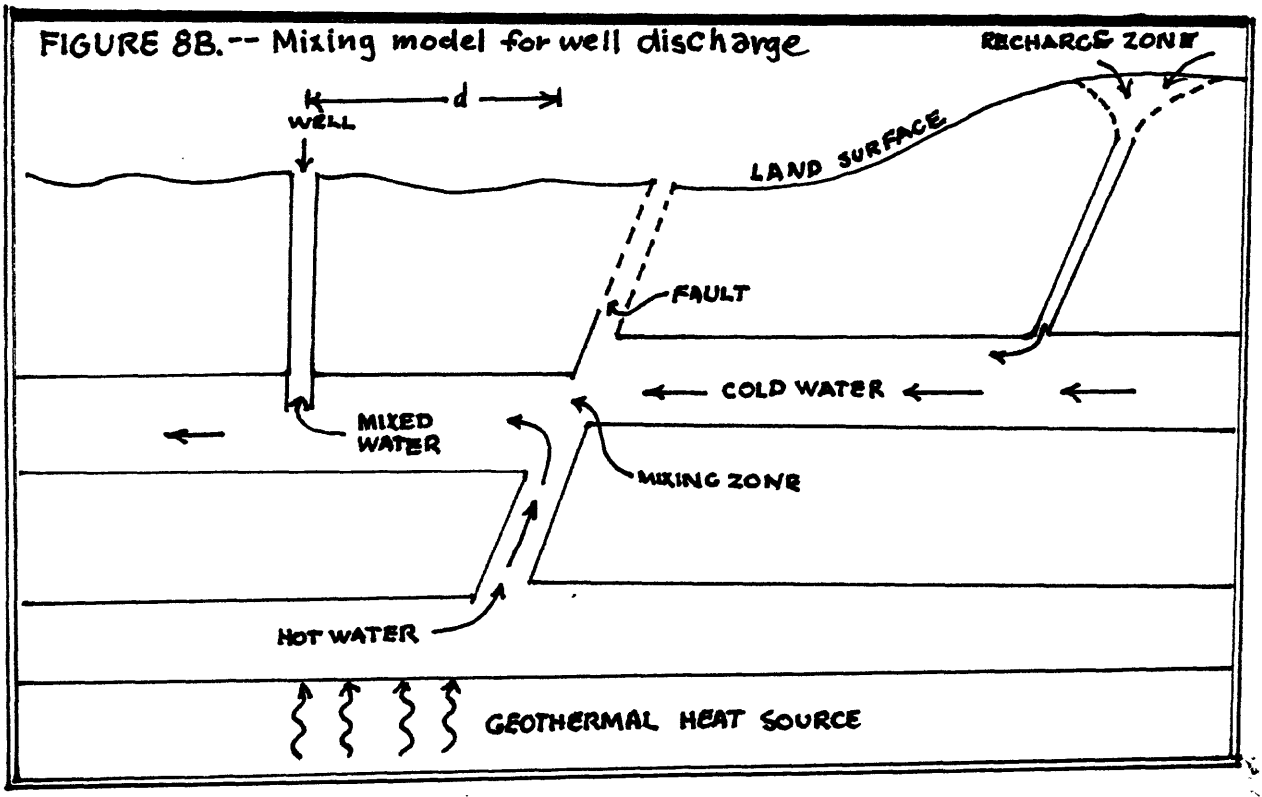

FIGURE 8. -- Schematic diagrams of mixing models

calculate the temperature and fraction of the hot-water component where the modes of mixing and discharge are conceptualized as shown schematically in figure 8A. In this model, hot water rises along a permeable channel, possibly a fault or joint. At some point the hot water encounters cold water from a permeable stratum. The cold water enters the hot-water channel and the mixture flows to the surface where it is discharged as a warm spring. The model of Fournier and Truesdell (1974) depends upon two assumptions: (1) The initial silica content of the deep hot water is controlled by the solubility of quartz and (2) no further solution or deposition of quartz occurs before or after mixing. These assumptions are valid when the residence time of the water in the reservoir is long and upward travel time is sufficiently short that even though the temperature of the water may decrease markedly, little chemical reequilibration can occur (Fournier and others, 1974). For the model shown in figure 8A, the data needed for the calculations are the temperatures and silica concentration of the cold-water before mixing, and those of the warm-spring discharge. The enthalpy of the hot water that heats the cold water is the same as the inital enthalpy of the deep hot water. Two equations can be written to solve for the two unknowns (the temperature of the hot water and the proportions of the hot and cold water) because the silica concentration and temperature of the warm spring are different functions of the original temperature of the hot water component (Fournier and Truesdell, 1974). The knowns in the equations include the temperature and the silica concentration of both the spring (or well) discharge as well as the cold-water component. Using tabular values of the heat content of liquid water and quartz solubilities, the equations can be solved graphically or on a computer, as described by Fournier, White, and Truesdell (1974) for the fractional component and premixing temperature of the thermal ground water.

A mixing model for the Stillwater area is shown in figure 8B. In this

model mixing occurs in the permeable stratum down qradient from the fault and discharge is from either a pumped or flowing well. The second assumption made for Fournier and Truesdell's (1974) model is somewhat more equivocal for this model. With increasing distance, d, of the well from the zone of mixing, the upward travel time, and thus the likelihood of further solution or deposition of silica, increases. Of course, the upward travel time is now a function of the lateral potential gradient and hydraulic conductivity of the permeable stratum, as well as d. With this in mind, the probable maximum subsurface temperature attained by the hot-water component and the proportions of the hot- and-cold-water components were computed for waters from CDDH's 117A and 123A and PW's 44 and 26. Results are shown below in table 9.

Temperature of the cold-water component was assumed to increase linearly with depth and its silica content was assumed to be constant areally. Calculated temperatures of the hot-water component range from 148 to 237°C. The two lowest temperatures bracket the minimum reservoir temperature of 159°C predicted by Mariner, Rapp, Willey, and Presser (1974) from quartz-silica geothermometry on the water from PW-26. The highest temperature of the hot-water component, 237°C, was calculated for PW-26. Fournier and Truesdell (1974) regarded estimates of subsurface temperature made using this model as probable maximum subsurface temperatures. Most evidence tends to support the reservoir temperature estimated by Mariner and the lower temperatures calculated using the mixing model. Specificially, the temperature of fluid from a 1,292 m geothermal test well near Stillwater reached a maximum of 156°C at 488 m, opposite a Tertiary (?) sandstone aquifer (W. F. Bueck, written communication, 1964). Thus, the mixing-model estimate of 237°C should be considered as a possible maximum reservoir temperature, with the actual temperature probably lying within the range of 150-170°C.

TABLE 9. -- Estimated maximum temperature of the hot-water component and fraction of cold-water component in mixtures of thermal and nonthermal ground waters.

Well or test hole number	Well discharge		Cold water component		Temp. of hot water component	Fraction of cold water
	Temp., °C	SiO_2, mg/L	Temp. °C [1/]	SiO_2, mg/L [2/]	°C	
PW-26A	95.7	170	16.3	37	237	0.65
PW-44A	94.0	120	15.4	37	187	0.55
DH-117A	66.6	80	12.5	37	164	0.64
DH-123A	46.4	58	13.2	37	148	0.75

Footnotes:

[1/] Estimate based on average regional temperature gradient of 75°C/km (Olmsted and others, 1975) and mean annual air temperature of 11°C.

[2/] Average silica concentration of test holes classified as "nonthernal". (See table 8.)

The dubious validity of some of the assumptions necessary to the well-discharge model and the many unknowns concerning the nature of the system make it important to use the results in table 9 with great caution in assessing the geothermal resource. For example, the temperature and silica concentration of the cold-water component at the point of mixing cannot be known with certainty. For this study an average "background" thermal gradient of $75^{o}C/km$ in the Quaternary fill was used to compute the temperature of the cold water. These computed temperatures are probably less than the actual temperatures, particularly if the "cold" component is heated significantly by conduction as it approaches the point of mixing. If the actual cold-water temperature is higher, the estimated temperature of the hot-water component would be too high. In addition, precipitation of silica is more likely to occur because of the extended travel time of the cooler, mixed water through the permeable stratum. Such a re-equilibration would cause the estimated temperature and proportion of the hot-water component to be too low. Similarly, the hot-water component itself may be a mixed water which has moved upward along a fault conduit after mixing with cooler water in a permeable statum at depth. The water discharged at the well-head may therefore be doubly or even triply mixed. Still, if significant re-equilibration has not occured, the temperature of the original hot-water component and its proportion could be estimated.

TEMPERATURE DISTRIBUTION AND HEAT FLOW

Temperatures and Temperature Gradients in Test Holes

Using the methods described previously in "Methods of Investigation," temperature logs were made in all test holes and soil temperature at a depth of 1 m was measured at 43 sites. A map of temperature at a depth of 30 m is shown in figure 9. The 30-m temperatures plotted in figure 9 were either measured directly, or where test holes were less than 30 m in depth, they were extrapolated using the average thermal gradient. Temperatures at 1 m were measured at each test-hole site and correlated with temperature at 30 m. The corresponding relation is plotted in figure 10. The linear least-mean-squares regression equation relating temperature at 30 m to temperature at 1 m is

$$T_{30} = 20.92\ T_1 - 223.95$$

where T_{30} is temperature at 30 m, T_1 is temperature at 1 m. The coefficient of determination, r^2 (a measure of the linearity of the relation) is 0.86, which indicates a reasonable fit to the regression for a temperature range of nearly 100°C at 30 m and 5°C at 1 m. Using the above equation, the 1-m temperature survey was used to delineate in greater detail the hottest parts of the thermal anomaly. The lines of equal temperature at 30 m were thus adapted from temperatures at 30 m in test holes and from temperatures at 1 m using the relationship shown in table 10 below. A map of temperature at 1 m is shown for comparison in figure 11. Prior to the 1-m temperature survey, little could be interpreted about the character of the central part of the thermal anomaly. The 20° and 30°C temperature pattern at 30-m depth revealed the anomaly to be elongated about a northwest-southeast axis, and it was assumed that a continuous central zone of high temperature extended along this axis. On the basis of the correlation with temperature at 1 m, however, there appear to be two distinct central highs alined along the axis with maximum temperatures at 30 m as great as 115°C.

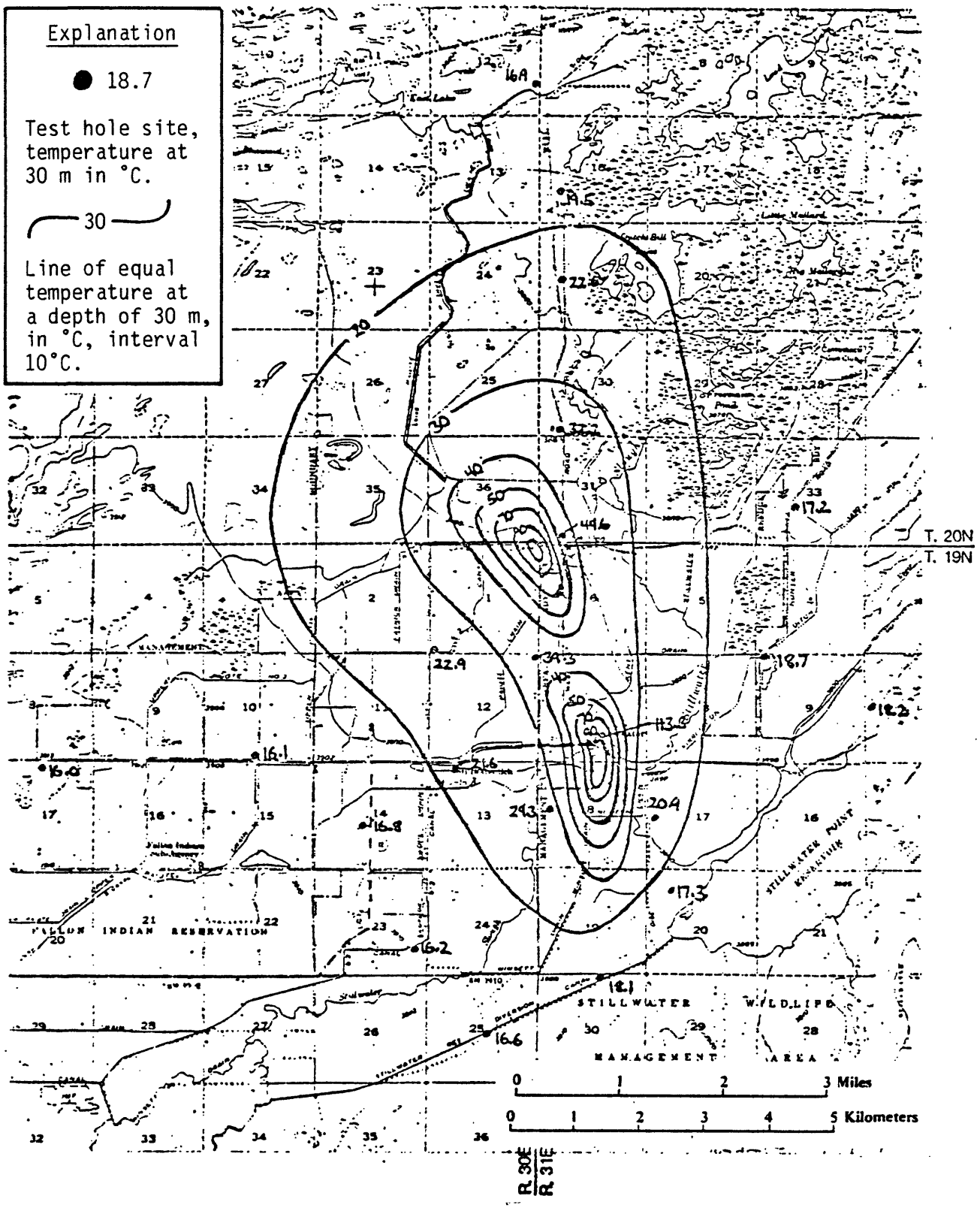

FIGURE 9. -- Temperature at a depth of 30 m

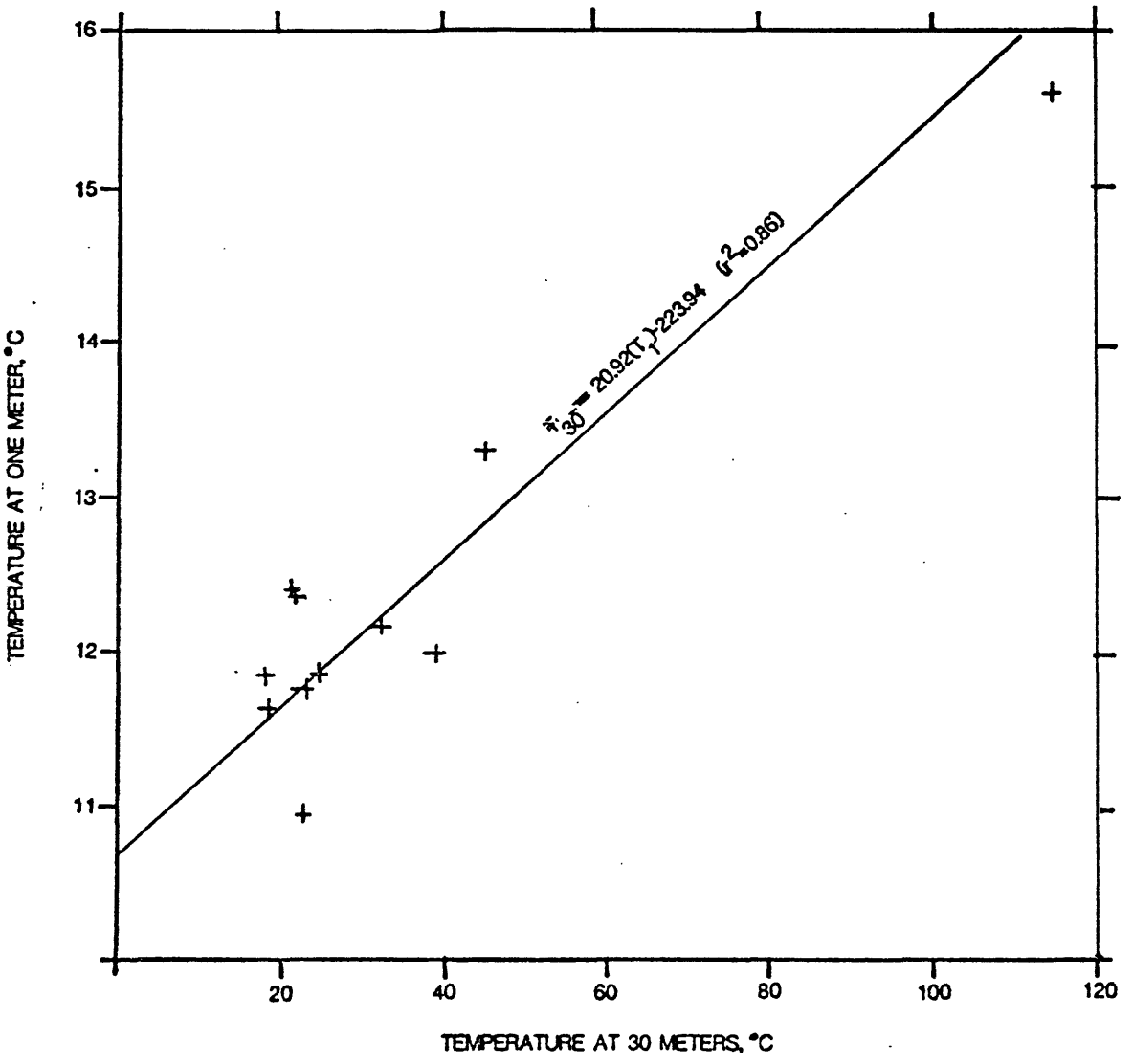

FIGURE 10. -- Correlation of temperature at a depth of 1 m with temperature at a depth of 30 m for 11 test holes

TABLE 10.-- Correlation of temperature at 30 m depth to temperature at 1 m depth, where:

$$T_{30} = 20.92\ T_1 - 223.95.\ ^{1/}$$

Temp. at 1 m, °C	Temp. at 30 m, °C	Rounded
11.0	6.2	10
12.0	27.1	30
13.0	48.0	50
14.0	68.9	70
15.0	89.8	90
16.0	110.8	110

Footnote:

1/ From linear least squares regression, shown in figure 10.

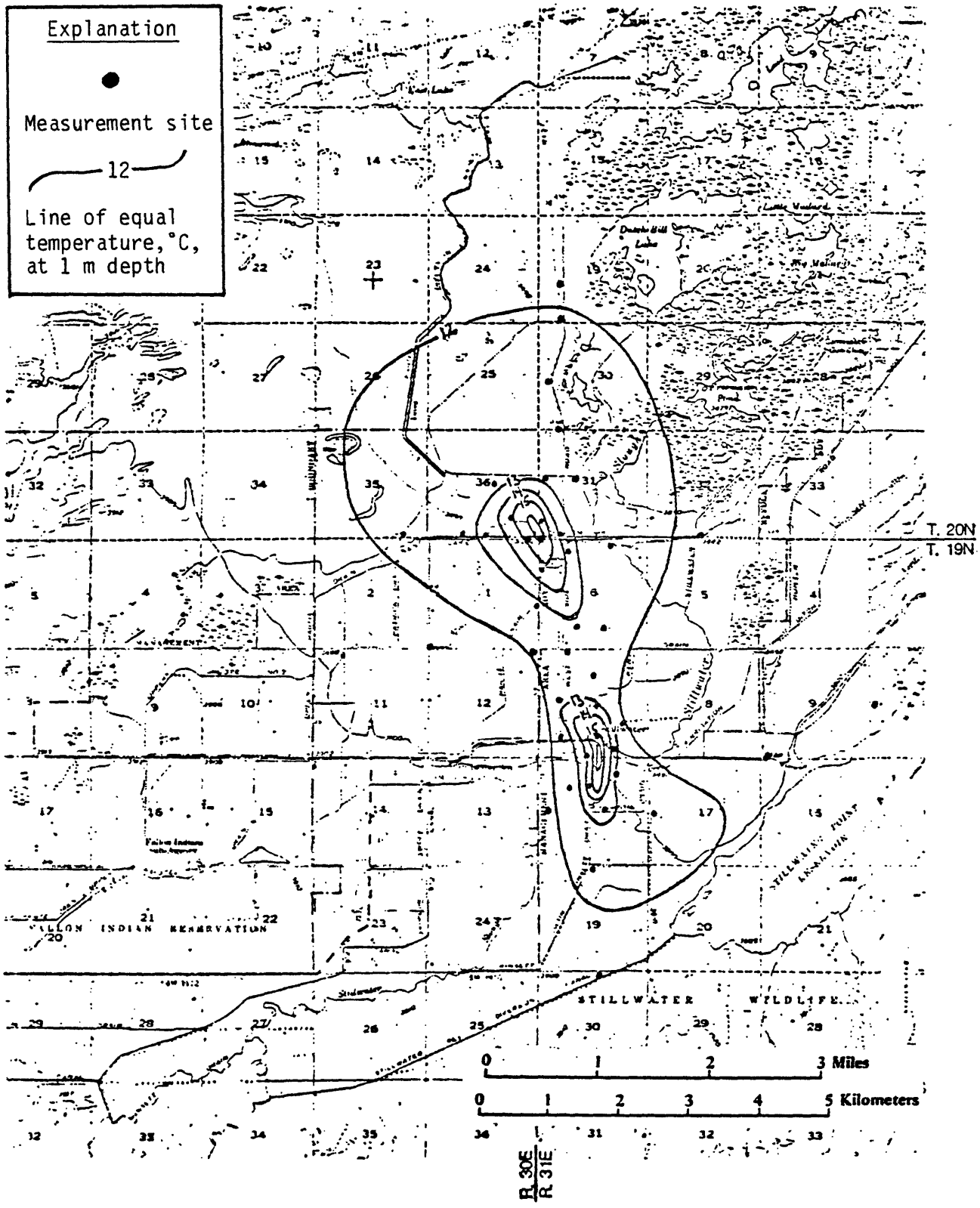

FIGURE 11. -- Temperature at a depth of 1 m, April 1978.

Data shown in plate 2 suggest that the two high-temperature zones are related to faults or zones of weakness in the deposits that transmit hot water upward by convection into shallow aquifers. This interpretation is supported by the temperature gradient of nearly 3,700°C/km measured in CDDH-117A near the middle of the southern high-temperature zone. As shown in plate 2, a fault is inferred very near CDDH-117A, and the test hole may indeed penetrate the fault plane. The rest of the temperature gradients are presumably conductive, ranging from 49° to 1,140°C/km.

Thermal Conductivity of the Materials

In order to calculate conductive heat flow, discussed in the next section, it is necessary to measure or estimate the thermal conductivity of the materials in which temperature gradients were measured. As discussed previously in "Methods of Investigation," 14 cores were analyzed for thermal conductivity by W. H. Somerton of the University of California, Berkeley, and three of these cores were later analyzed by Robert Munroe of the U.S. Geological Survey in Menlo Park. The results of these analyses (those by Somerton included saturated bulk density, dry bulk density, porosity, and grain density) are presented in table 11.

Thermal-conductivity measurements by Somerton's laboratory were made with a steady-state comparator (divided-bar) apparatus; those by Munroe's laboratory were made with a needle-probe apparatus. The three samples measured by Munroe were from the same cored intervals but were not the same samples as those measured by Sommerton. The values obtained by Munroe range from 7 to 34 percent and average 20 percent less than those obtained by Somerton. Although part of the difference could result from variability within the cored intervals, the two measurement techniques probably yield different results for the same materials, as discussed below.

TABLE 11.-- Core data from test holes in the Stillwater KGRA, Churchill County, Nevada [1/].

Test hole number	Depth interval (m)	Matrerial	Saturated bulk density (g/cm^3)	Dry bulk density (g/cm^3)	Porosity (Frac.)	Temperature of thermal conductivity measurement (^oC)	Thermal conductivity [2/] (mcal/cm s^oC)	Grain density (g/cm^3)	Grain thermal conductivity [3/] (mcal/cm s^oC)
DH-101A	30.48-31.24	Clay, silty with fine sand	1.90	1.49	0.44	51.7	3.93	2.66	8.25
DH-102A	153.0-153.8	Clay, silty	1.60	1.14	0.58	51.7	3.05	2.71	7.91
DH-106A	18.7-19.5	Sand, fine, silty	1.93	1.59	0.41	48.9	3.93	2.69	7.57
DH-106C	81.7-82.5	Sand, fine, silty	2.03	1.70	0.37	52.2	4.20	2.70	7.60
DH-107A	21.6-22.4	Clay	1.63	1.10	0.59	51.4	2.70	2.68	6.11
DH-107A	32.8-34.6	Sand, clay	1.98	1.60	0.41	51.7	4.42	2.71	9.24
DH-107A	45.0-45.8	Sand, medium	2.03	1.71	0.37	52.2	4.93 (3.27)	2.71	9.80 (5.10)
DH-110A	20.9-21.7	Sand, medium	1.92	1.53	0.44	51.7	3.71	2.73	7.44
DH-112A	55.2-56.0	Clay, shaley	1.40	0.59	0.67	52.2	2.27 (2.11)	1.79	5.00 (4.40)
DH-113A	74.9-48.7	Sand, medium-coarse with clay	1.93	1.55	0.43	50.6	4.44	2.72	4.92
DH-116A	14.5-15.3	Clay	1.32	0.56	0.76	53.9	2.38	2.33	9.64
DH-117A	21.3-22.1	Sand, medium, silty	1.90	1.50	0.40	50.0	4.38 (3.55)	2.50	8.83 (6.21)
DH-119A	18.7-19.5	Sand, fine	1.90	1.50	0.45	51.5	4.20	2.73	9.60
DH-122A	19.5-20.3	Silt, sandy	1.92	1.56	0.43	50.8	4.38	2.72	9.68

Footnotes:

[1/] Except where noted, analyses done by W. H. Somerton's laboratory, at the University of California at Berkeley, thermal conductivity measured using steady-state comparator, May 1978.

[2/] Figures in parenthesis indicate Thermal conductivity measured at U.S. Geological Survey laboratory, Menlo Park, CA by Robert Munroe using needle probe, July 1978.

[3/] Figures in parenthesis calculated from Somerton's porosity data and R. Munroe's thermal conductivity data.

Actual measured values of thermal conductivity for only 14 core samples obviously were insufficient to use directly for calculating heat flow for an aggregate of several hundred meters depth of temperature-gradient measurements. Instead, estimated values of thermal conductivity were assigned to various categories of materials described in the logs of the test holes in a manner similar to that described by Olmsted, Glancy, Harrill, Rush, and Van Denburgh (1975, p. 62-64). The values listed in table 12 are not based on the data from Somerton's laboratory (table 11) but are based on 93 needle-probe measurements of thermal conductivity of 40 cores for a study in progress by the U.S. Geological Survey (F. H. Olmsted, written communication, 1978). The values obtained by Munroe for the three samples from Stillwater are in good agreement with the earlier needle-probe values for similar deposits but are systematically less than the values obtained by Somerton's laboratory with the divided-bar apparatus.

Although the issue of which measurement technique furnishes the more accurate results cannot be resolved with data presently at hand, it was decided to use the values based on the needle-probe measurements (table 12). The reason for this choice is that the heat-flow values calculated for Stillwater therefore can be compared directly with values from the western Carson Desert and also from several other localities in northern and central Nevada for which data based on needle-probe measurements are available. The heat-flow estimates for the Stillwater area can be modified at any time on the basis of a need to adjust the values of thermal conductivity assigned in this study. The values listed in table 12 are believed to be well within 30 percent of the correct values of thermal conductivity of the materials in which temperature gradients were measured.

TABLE 12.-- Values of thermal conductivity assigned to lithologic categories classified in interpreted logs.

Lithologic category [1/]	Thermal conductivity (mcal cm^{-1} s^{-1} $^{o}C^{-1}$)
Gravel; gravel and sand; sandy gravel	5.0
Sand and gravel; gravelly sand; sand, silt, gravel; gravel and sand	4.0
Medium sand; fine to medium sand; coarse sand with some clay and silt	3.5
Fine sand; silty sand; sand and silt; sand and clay; clay and gravel	3.0
Silt and fine sand; clay and fine sand	2.5
Clay, silty clay; clay and silt; silt and clay	2.0

Footnote:

[1/] Assumed to be fully saturated.

Heat Discharge

All geothermal heat is assumed to be discharged from the area by convection as flow from the many domestic heating wells and by conduction through near-surface sedimentary deposits. Nowhere in the area is heat discharged by natural spring flow, by steam from fumaroles, or in significant quantities by radiation. Potentially, heat may be discharged by lateral ground water flow; however, the boundary of the area for which discharge is calculated is the 3 hfu isogram which is very near background or "normal" heat discharge. Therefore convective discharge by lateral ground water movement beyond the boundary of the thermal area is small and is neglected.

Heat flux by discharge from local geothermal heating wells is small in comparison to that by conduction, but is significant in terms of the total net heat discharge for the area.

There are approximately 30 domestic wells in the Stillwater area that are used exclusively for space heating. Each well is estimated to either flow or be pumped at an average annual rate of 1 L/s with an average discharge temperature of $70^{o}C$. Convective heat discharge is calculated as follows:

Average temperature of well discharge	$=70^{o}C$.
Enthalpy of well discharge	=70 cal/g
Mean annual temperature at land surface	$=11^{o}C$
Enthalpy at land surface	=11 cal/g
Net enthalpy of well discharge	=59 cal/g
Well discharge	=30 L/s
Density of water at $70^{o}C$	$=0.977\ g/cm^3$

$$\text{Heat discharge} = (59\ cal/g)(0.977\ g/cm^3)(30 \times 10^3\ cm^3/s)$$
$$= 1.7 \times 10^6\ cal/s$$

Although rough, the above estimate is considered to be conservative. A catalog of flow rates and temperature of heating wells in the area probably would yield

a somewhat higher estimate.

Where temperature gradients are linear, that is, temperature increases with depth at a constant rate through material of uniform thermal conductivity, heat flow is inferred to be by conduction and is computed as the product of the thermal conductivity and the temperature gradient. Near-surface conductive heat flow was computed at the site of each test hole as follows. The lithologic log for each test hole was interpreted using the drilling log and geophysical logs. Values of thermal conductivity were then assigned to the various lithologic categories (types of material) according to table 12.

From the plots of temperature vs depth, linear least-mean-squares temperature gradients were computed for one or more intervals, depending on the shape of the curve. Only one discernible slope (gradient) was observed in the shallower test holes. In the deep holes gross changes in lithology (and thermal conductivity) were reflected by changes in the slope of the temperature-depth curve (that is increasing gradients in zone of low thermal conductivity and vice versa). Within the interval of each linear portion of the temperature-depth curve, thermal conductivities should be roughly uniform; in practice, these intervals contained thin-bedded materials of contrasting thermal conductivity. To account for this, the harmonic-mean thermal conductivity of the beds within each interval was calculated. The harmonic-mean thermal conductivity for a series of n geologic layers is computed as

$$K_m = \sum_{i=1}^{n} \frac{z_i}{z_i/K_i}$$

where z_i equals the thickness of layer i and Ki equals the thermal conductivity of layer i.This value was multiplied by the linear least-mean-squares thermal gradient to obtain conductive heat flow through the interval. Ideally, the heat flow through all the intervals would be equal; in application they differed by as much as 20 percent. Total heat flow at any test hole was

computed as the arithmetic mean of the discharges through each interval.

The heat-flow values from the test holes of this study and those from the the test holes of the previous study (Olmsted and others, 1975) were used to construct a heat-flow map (fig. 12). In addition, temperatures at depth of 1 m at test-hole sites were correlated with heat flow and used to delineate the area of the highest heat flow, much as they were used to delineate heat-flow patterns by Sass, Ziagos, Wollenberg, Monroe, de Somma, and Lachenbruch (1977), who correlated temperature at 15 m with heat flow near the Leach Hot Springs area, Grass Valley, Nevada. The possibility of large error is, of course, introduced by correlating heat flow with temperature within the zone of seasonal fluctuation. Nonetheless, the relationship of temperature at 1 m to heat flow is approximately linear as illustrated by figure 13. The linear least-mean-squares regression equation is $Q = 16.30\ T_1 - 184.10$ where Q is heat flow (in hfu) and T_1 is temperature (^{o}C) at 1 m. The coefficient of determination, r^2, is 0.83.

Heat discharge from the area between two heat-flow isograms was computed as the product of the area between the two isograms and the geometric mean of the two isograms. The heat discharges from the areas between the heat-flow isograms were then added to obtain the total conductive heat discharge from the thermal area. This estimate is derived below in table 13.

It is instructive to compute the net conductive heat discharge at the land surface that results from the convective upflow and subsequent lateral flow of thermal ground water. The calculation is made by substracting the so-called "normal heat discharge for the area-- the heat that would have been discharged at the surface without a convective system-- from the total conductive heat discharge given in table 13. For the purpose of the estimate, it is assumed that "normal" heat flow for the Carson Desert is 3 hfu, the value used in defining the outer limit of the thermal anomaly. The normal conductive heat flow within the 3 hfu isogram is equal to

$$(3 \times 10^{-6} cal/cm^2 s)(100.6 \times 10^{10} cm^2) = 3.0 \times 10^{6}\ cal/s$$

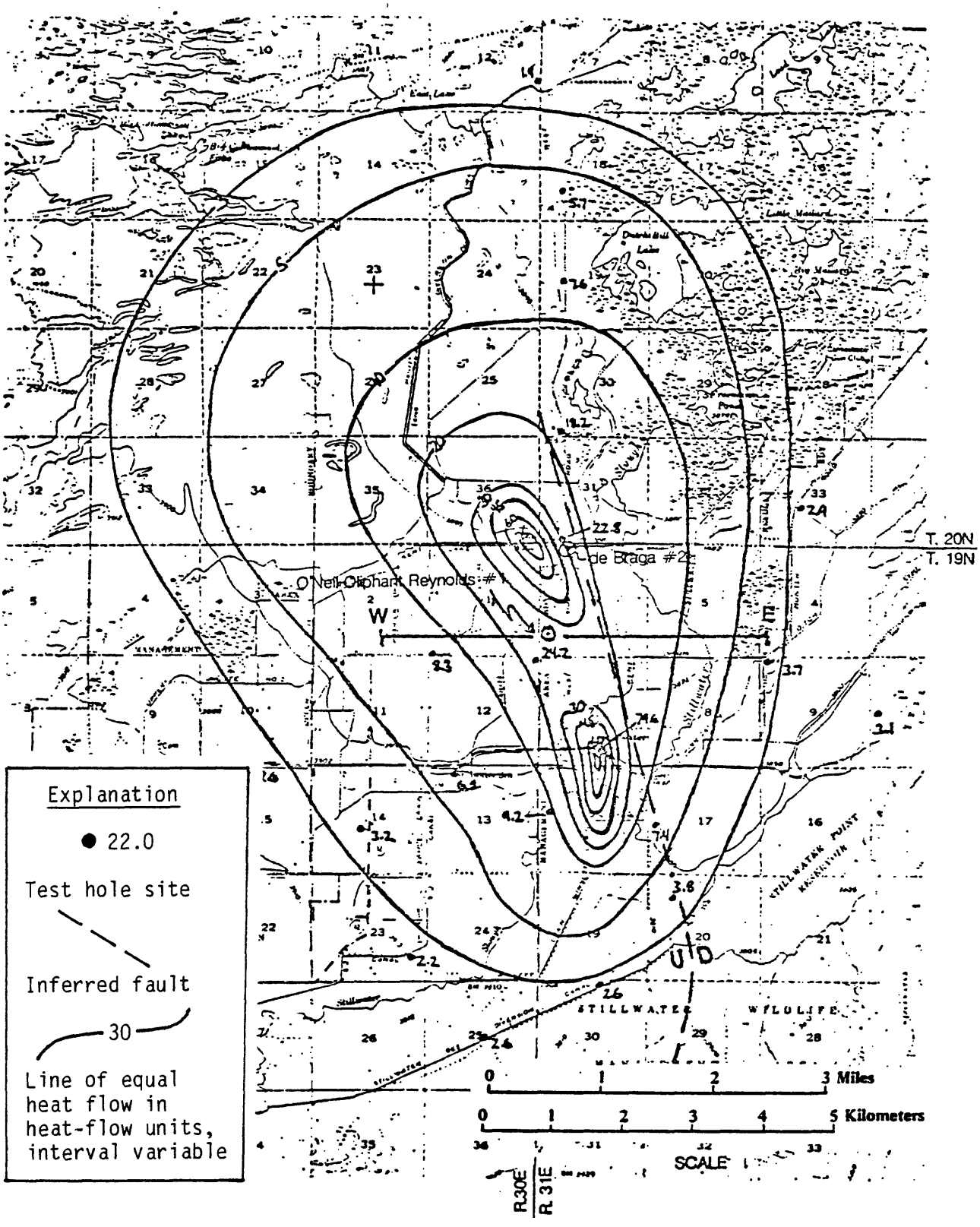

FIGURE 12. -- Estimated near-surface conductive heat flow

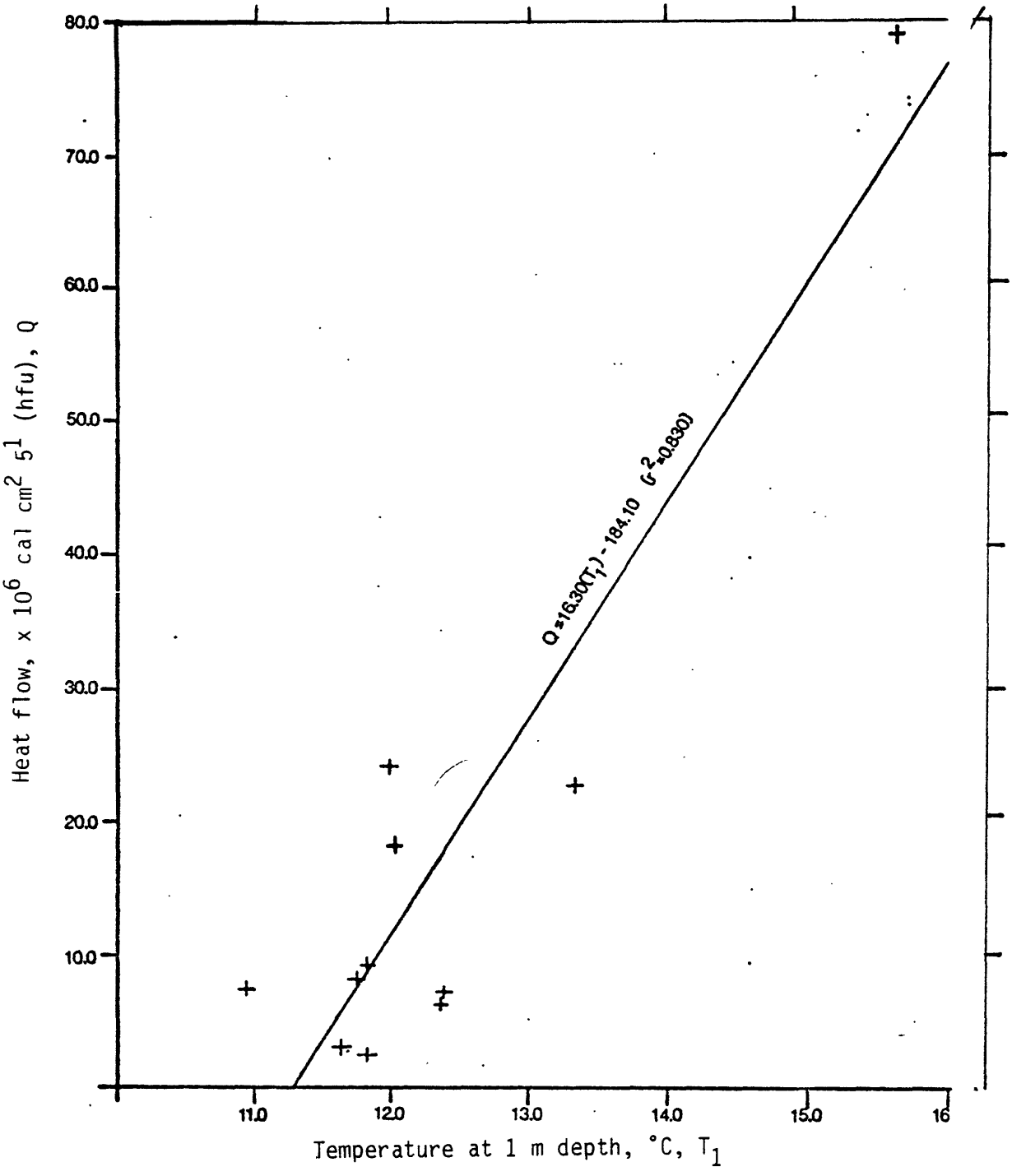

FIGURE 13. -- Correlation of heat flow and temperature at a depth of m for 11 test holes.

TABLE 13.-- Estimate of near-surface conductive heat discharge from the Stillwater geothermal area.

Range in heat flow ($\times 10^{-6}$ cal/cm^2 s)	Area enclosed ($\times 10^{10}$ cm^2=km^2)	Geometric mean heat flow ($\times 10^{-6}$ cal/cm^2 s)	Heat discharge ($\times 10^6$ cal/s)
3-5	35.8	3.9	1.4
5-10	42.6	7.1	3.0
10-20	12.5	14.1	1.8
20-30	6.4	24.5	1.6
30-45	1.5	36.7	0.6
45-60	1.1	52.0	0.6
60-75	0.4	67.1	0.3
above 75	0.3	75.0	0.2
total =	100.6	total =	9.5

and excess conductive heat discharge is equal to

$$9.5 \times 10^6 \text{ cal/s} - 3.0 \times 10^6 \text{ cal/s} = 6.5 \times 10^6 \text{ cal/s}$$

The total thermal discharge from the area is then,

excess conductive discharge, 6.5×10^6 cal/s

+ convective discharge, from wells, 1.7×10^6 cal/s

= total heat discharge, 8.2×10^6 cal/s.

The above estimate is regarded as reasonably accurate. If anything, the estimate probably is too low. Convective upflow may affect shallow gradients in the central part of the anomaly, so that the assumption of linear conductive gradients leads to heat-flow values that are too low. Olmsted, Glancy, Harrill, Rush, and Van Denburgh (1975) neglected convective discharge from wells and made several simplifying assumptions in computing an excess conductive heat discharge of 14×10^6 cal/s. This estimate was also considered to be conservative and for the same reasons described above. The difference in these estimates is nearly a factor of two and can be largely attributed to the increased resolution of heat-flow distribution in the central part of the thermal anomaly attained from additional data collected for this study.

Relation of Near-Surface Heat Flow to Ground-Water Movement

The pattern of heat flow shown in figure 12 is related to two factors. The strong northwest-southeast lineation of the central part of the thermal anomaly is no doubt related to similar lineation of the thermal conduit or conduits. The asymmetrical inverted tear-drop shape of the anomaly is directly attributable to lateral transport of heat by shallow ground-water flow. The net movement of ground water within the upper 30 m is north and slightly east; the northwest trend of the anomaly thus reflects the dominance of the conduit lineation. Also, the more rapid decrease in heat flow toward the east may be due to net ground-water recharge from the nearby alluvial apron of the Stillwater Range.

Heat Budget

The purpose of the heat budget presented here is to estimate the volume of thermal ground water rising from the geothermal reservoir. The overriding assumption used in the calculation is that all heat discharged by the system in excess of normal conductive heat flow is transported by upflowing thermal ground water. In addition, the following assumptions are made:

(1) The shallow part of the hydrothermal system is in hydrologic and thermal equilibrium.

(2) Water temperature at the deep source is accurately reflected by geothermometry and the temperature of the deep source at Stillwater is 159°C as determined by Mariner, Rapp, Willey, and Presser (1974) using the silica-quartz geothermometer.

(3) The rising thermal ground water leaves the deep source at the temperature indicated by the geothermometer.

Using these assumptions thermal discharge is computed as follows: Enthalpy of water leaving deep source = $(159^{\circ}C)(1.0\ cal/g) = 159\ cal/g$.

Enthalpy of water discharged at land surface = $(11^{\circ}C)(1.0\ cal/g) = 11\ cal/g$)

Net enthalpy of discharge = 148 cal/g.

Total heat discharge = 8.2×10^6 cal/s.

Discharge of thermal water

$$= \frac{8.2 \times 10^6 \text{ cal/s}}{1.48 \times 10^2 \text{ cal/g}} = 55 \text{ kg/s}$$

Therefore, approximately 55 kg/s of water leave the geothermal reservoir at 159°C and carry 2.6×10^{14} cal/yr of heat. About 21 percent of this heat is discharged convectively from wells, the remainder by conduction through near-surface deposits. This estimate of the thermal water upflow is approximately one half the value obtained by Olmsted, Glancy, Harrill, Rush, and Van Denburgh (1975) on the basis of a total heat discharge of 16×10^6 cal/s.

CONCEPTUAL MODEL OF THE HYDROTHERMAL SYSTEM

A generalized conceptual model of the Stillwater hydrothermal system is shown in the diagrammatic section in figure 14. (See fig. 12 for location of the section.) The model is similar to that proposed in an earlier study by Olmsted, Glancy, Harrill, Rush, and Van Denburgh (1975) and also to others proposed for hydrothermal systems in the Basin and Range province (see Welch and others, 1981). It is based chiefly on data from shallow ($\leq$ 152 m) test drilling at 14 sites for the present study and 10 sites for the earlier study (Olmsted and others, 1975), from the O'Neil-Oliphant Reynolds No. 1 and Union de Braga No. 2 geothermal test wells, from gravity and magnetic surveys, and from geologic data from several sources.

The principal features of the model are summarized as follows. The hydrothermal system results from deep circulation of meteoric water. The cold meteoric recharge water presumably moves downward along a fault or system of faults to a permeable zone or zones--the "geothermal reservoir"--within consolidated rocks of the Tertiary and (or) pre-Tertiary age. As the water moves laterally through the "reservoir" it is heated by capturing part of the regional heat flow. Hot water eventually leaves the "reservoir" and rises along a steeply dipping basin-and-range fault or fault system. Much of the rising thermal water discharges laterally into a sand aquifer of probable Tertiary age but some of it rises into overlying Quaternary deposits and discharges laterally into sands within these deposits. Discharge of hot water at the surface is prevented, however, by the absence of fault conduits within the uppermost deposits, some of which have extremely low vertical hydraulic conductivity.

Circulation of water in this system is driven by (1) density gradients that develop as the cold water is heated, resulting in convective flow, and (2) potential gradients that result from the higher altitude of the recharge areas

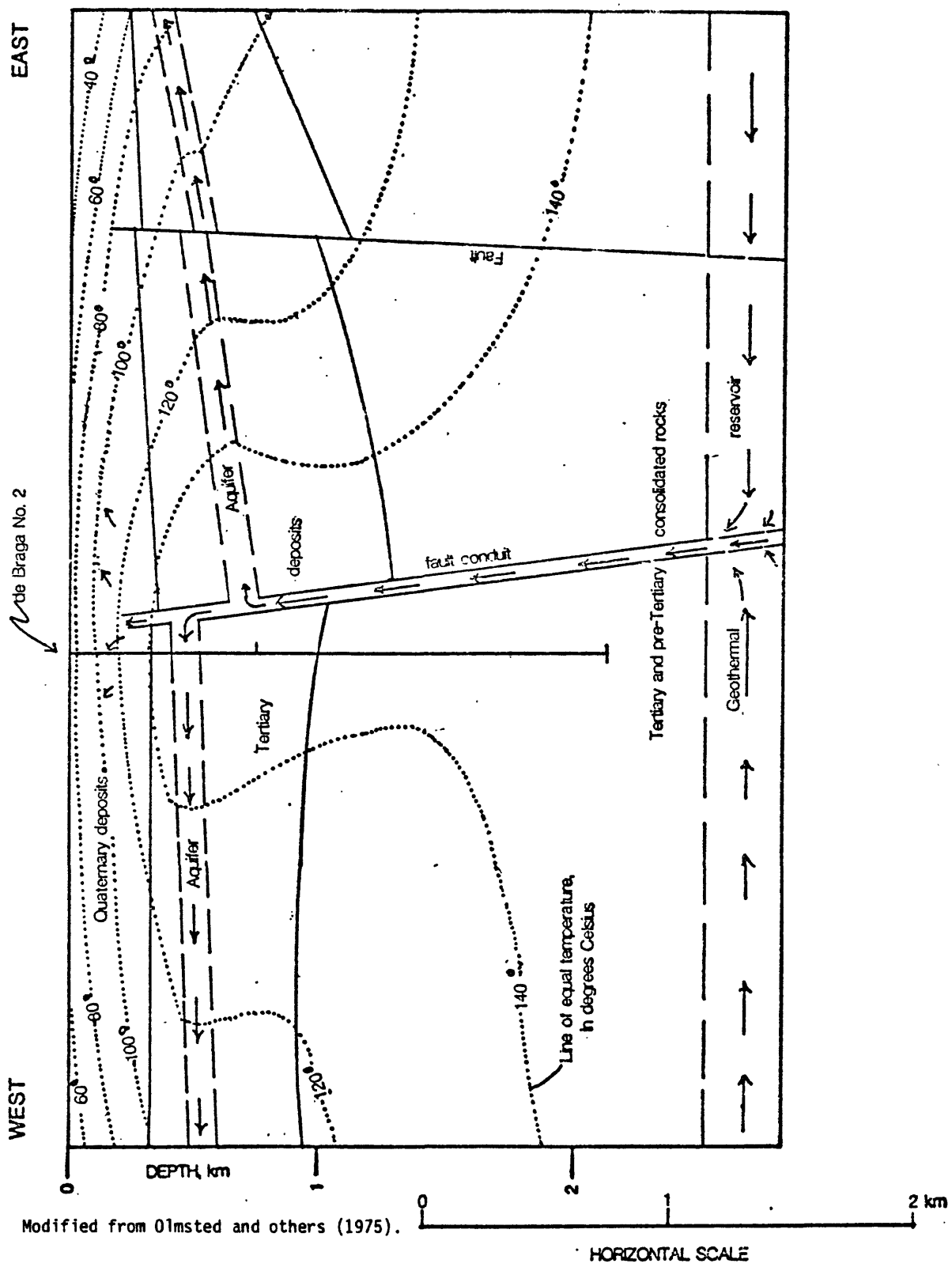

FIGURE 14. -- Conceptual model of the deep hydrothermal discharge system.

relative to the discharge areas. The relative magnitude of these two driving forces cannot be determined because of uncertainties as to the location of the recharge areas and the maximum temperatures attained by the thermal water in the deepest part of the flow system.

The source of heat for the Stillwater hydrothermal system cannot be identified unequivocally from present information. Magnetotelluric and aeromagnetic data reveal an extensive low-resisitivity ($\leq 1\Omega$ -m) layer at depths of 2.5-7 km. This layer has been interpreted in two ways: (1) as a geothermal reservoir containing hot brine (Stanley and others, 1976), which tends to support a deep-crustal heat-source model, or (2) as a shallow-crustal heat source consisting of magma or partly molten crust (UURI release STIL UOC-2, 3). Other evidence, such as anomalously thin (24-km) crust in the region indicated by seismic-refraction data (Pakiser and Hill, 1963) and moderately low heat-flow values outside the thermal anomaly (Olmsted and others, 1975; Sass and others, 1977), suggest that the hydrothermal system is most likely a result of deep circulation of meteoric water and convective upflow in an area of perhaps somewhat above-normal basin-and-range heat flow.

Temperature data from the de Braga No. 2 geothermal test well (UURI release STIL UOC-2, 3) corroborate the conceptual model shown in figure 14. The de Braga well is 1.3 km north of the O'Neil-Oliphant Reynolds No.1 well (fig. 12). Variation in temperature with depth in the de Braga well is shown in figure 15. The boundaries between units in the stratigraphic column to the right of the temperature profile, which is based on data from the Reynolds No.1 well (shown in fig. 14), agree closely with the breaks in the temperature profile. The high temperature gradient in the upper part of the profile reflects the low thermal conductivity and the conductive thermal regime within the upper 400 m of unconsolidated Tertiary and Quaternary deposits.

White, D. E., 1970, Geochemistry applied to the discovery, evaluation, and exploration of geothermal energy resources: U.N. Symposium on the development and utilization of geothermal resources, Pisa, Geothermics, Special Issue 2, v.1, p. 58-80.

Willden, Ronald, and Speed, R. C.,1974, Geology and mineral deposits of Churchill County, Nevada: Nevada Bureau of Mines, Bulletin 83.

Wollenberg, H. A., Bowman, H.,and Asaro, F., 1977, Geochemical studies at four northern Nevada hot spring areas: Lawrence Berkeley Laboratory, University of California, Berkeley, LBL-6808, 69 p.